



Auckland
Regional Council
TE RAUHITANGA TAIAO

Evidence for the physical effects of
catchment sediment runoff
preserved in estuarine sediments:
Phase II (field study)

December 2002 Technical Publication 221

Auckland Regional Council
Technical Publication No. 221, December 2002
ISBN 1-877353-25-6, ISSN 1175 205X
www.arc.govt.nz

on recycled paper

Evidence for the physical effects of catchment sediment runoff preserved in estuarine sediments: Phase II (field study)

A. Swales
T. M. Hume
M. S. McGlone¹
R. Pilvio²
R. Ovenden
N. Zviguina¹
S. Hatton
P. Nicholls
R. Budd
J. Hewitt
S. Pickmere
K. Costley

(1) Landcare Research Ltd, Lincoln
(2) National Radiation Laboratory, Christchurch

Prepared for
Auckland Regional Council

NIWA Client Report: HAM2002-067
December 2002
NIWA Project: ARC01272

National Institute of Water & Atmospheric Research Ltd
Gate 10, Silverdale Road, Hamilton
P O Box 11115, Hamilton, New Zealand
Phone +64-7-856 7026, Fax +64-7-856 0151
www.niwa.co.nz

Contents

Executive Summary	iv
1. Introduction	1
1.1 Background	1
1.2 Limitations of present knowledge	2
1.3 Study objectives	3
2. Methods	5
2.1 Rationale	5
2.2 Dating of recent estuarine sediments	9
2.2.1 Pollen dating	10
2.2.2 Radioisotope dating	15
2.3 Sedimentation rates	22
2.4 Sediment coring	25
2.5 Laboratory analyses	25
3. Results	29
3.1 Estuary and catchment characteristics	29
3.2 Mahurangi estuary (intertidal and sub-tidal cores)	30
3.2.1 Background	30
3.2.2 Mahurangi estuary sediments	32
3.2.3 Mahurangi recent sedimentation history	34
3.3 Puhoi estuary (intertidal cores)	41
3.3.1 Background	41
3.3.2 Puhoi estuary sediments	43
3.3.3 Puhoi recent sedimentation history	44
3.4 Okura estuary (intertidal cores)	47
3.4.1 Background	47
3.4.2 Okura estuary sediments	49
3.4.3 Okura recent sedimentation history	51
3.5 Henderson creek (intertidal cores)	58
3.5.1 Background	58
3.5.2 Henderson estuary sediments	60
3.5.3 Henderson creek recent sedimentation history	62
3.6 Waitemata-Te Atatu (sub-tidal cores)	65
3.6.1 Background	65
3.6.2 Waitemata sub-tidal sediments	65
3.6.3 Waitemata (sub-tidal) recent sedimentation history	67
3.7 Whitford embayment (sub-tidal cores)	70
3.7.1 Background	70
3.7.2 Whitford sediments	72
3.7.3 Whitford recent sedimentation history	73
3.8 Wairoa estuary (intertidal and sub-tidal cores)	77
3.8.1 Background	77
3.8.2 Wairoa estuary sediments	79
3.8.3 Wairoa recent sedimentation history	82
3.9 Te Matuku estuary (intertidal cores)	91
3.9.1 Background	91
3.9.2 Te Matuku sediments	92
3.9.3 Te Matuku recent sedimentation history	93

4.	Recent sedimentation in Auckland estuaries	101
4.1	Comments on physical indicators	101
4.2	Comparison of pollen, ¹³⁷ Cs and ²¹⁰ Pb SAR	107
4.3	Inter-core replication	108
4.4	Comparison of SAR between estuary sub-environment	109
4.5	Physical similarity of estuaries	111
5.	How Auckland estuaries are impacted by catchment sediment loads	115
5.1	Estuary types and environments	115
5.2	How estuaries infill with sediment and age	115
5.3	Factors that accelerate the aging process	117
5.4	Sedimentation in different types of estuaries	117
5.5	Historical changes in estuary sedimentation	122
5.6	What does the future hold ?	126
6.	Acknowledgements	129
7.	References	131
8.	Appendix I: Table of GPS Co-ordinates for sediment core locations	139
9.	Appendix II: Auckland estuaries cores: depth profiles of pollen and spore abundance by (1) major plant types and (2) detailed diagrams with scientific names to <i>Genus</i> or <i>species</i> level.	141
10.	Appendix III: Estuary sediment cores: ²²⁶Ra Concentration profiles	171
11.	Appendix IV: Estuary sediment cores: dry bulk sediment density (gcm⁻³) profiles	174

Executive Summary

Catchment development increases sediment loads delivered to estuaries during earthworks and in urban areas contaminant loads increase as urban areas mature. While some of this sediment and contaminant load is discharged to the sea, part of this load is trapped in estuaries. Evidence for the effects of catchment sediment runoff is preserved in estuarine sediments. By examining the stratigraphic record in sediment cores (the sequence and composition of sediment deposits) we are able to determine the effects of human activities on these systems.

In an earlier report (Hume et al. 2002) we identified preferred methods and indicators to determine the physical effects of catchment sediment loads on estuaries. This report builds on that earlier work. The study objectives are to: (1) reconstruct a regional snapshot of the present physical condition and recent sedimentation history (i.e., last 50 years) of Auckland estuaries; (2) document empirical evidence for the effects of catchment soil erosion on a range of estuary habitats; (3) identify potential State-of-the-Environment physical indicators for estuaries; (4) provide empirical data to support numerical model predictions of estuary sedimentation associated with past (hindcast) and likely future (forecast) catchment development; (6) develop a conceptual physical model of how Auckland's estuarine systems will likely be impacted by future catchment sediment runoff.

Previous studies of sedimentation in Auckland estuaries have focused on the tidal creeks near catchment outlets. To address this imbalance in our knowledge of Auckland estuaries, we focus on sub-tidal and intertidal flat environments in the main body of estuaries. Also, importantly, the diversity of benthic macrofaunal communities living in these environments is typically greater than in tidal creeks. These benthic fauna are generally more adversely affected by fine sediment runoff than tidal-creek fauna.

Sediment cores were collected (Fig. A) from drowned-valley estuaries (Mahurangi -6 sites, Okura -3 sites, Waitemata -3 sites, Henderson -3 sites, Wairoa -6 sites), tidal lagoons (Puhoi -3 sites) and coastal embayments (Whitford -3 sites, Te Matuku - Waiheke Island -3 sites). Sediment cores were dated using pollen, caesium-137 (^{137}Cs) and lead-210 (^{210}Pb). Zinc (Zn) concentrations in the cores were measured to identify urban sediments. Sediment particle size was also determined to assess the types of sediment being deposited in different types of estuaries and sub-environments.

Key findings and contributions are:

- The sediment accumulation rate (SAR) is a key State-of-the-Environment physical indicator of the effects of catchment use change in estuaries. Complimentary and independent dating of estuarine sediments is of critical importance to ensure the reliability of SAR estimates. Our studies show that sediment Zn concentration and mud content in addition to pollen, ^{137}Cs and ^{210}Pb dating are valuable in this respect.

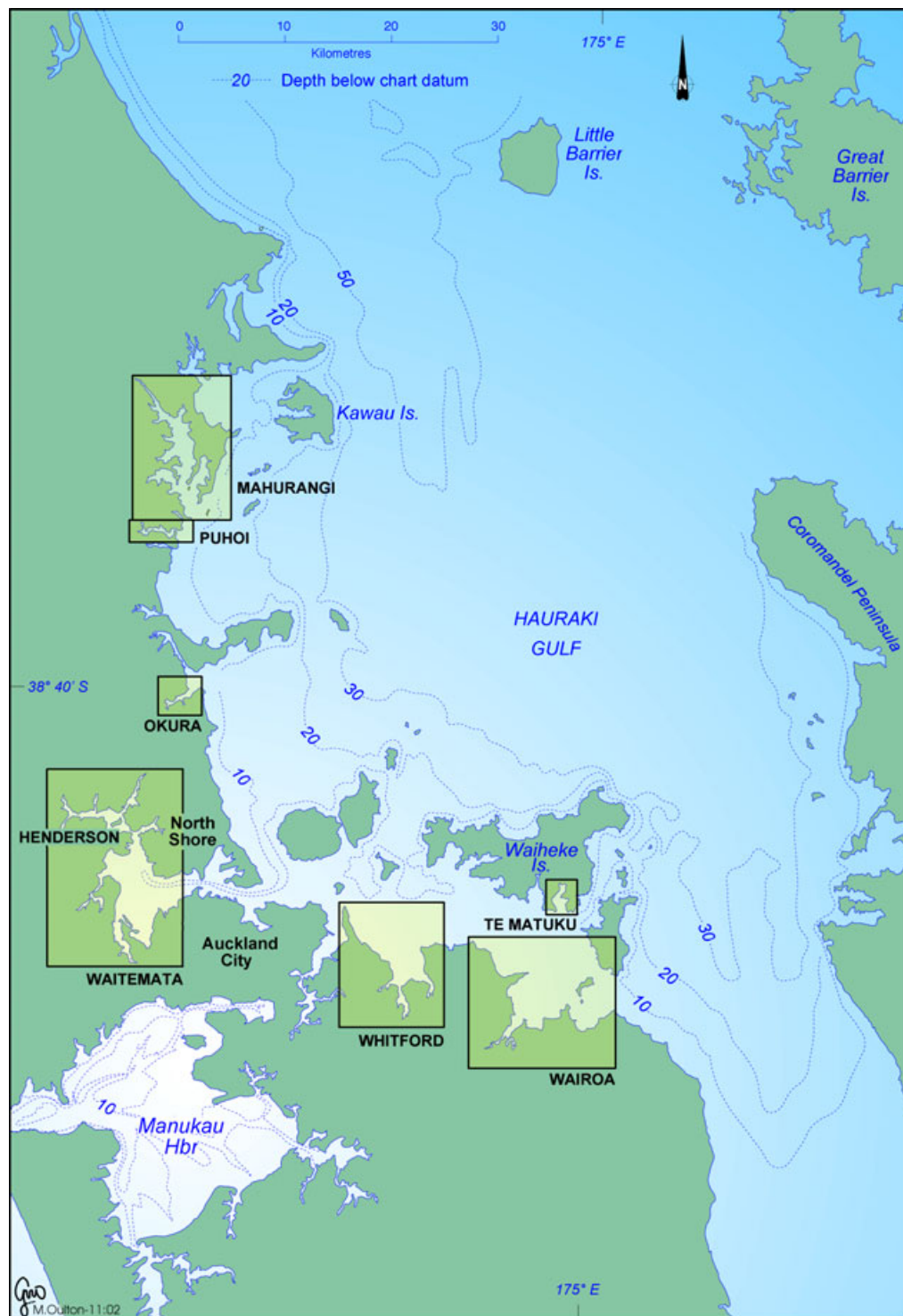


Figure A: Auckland estuaries selected for the regional sedimentation study.

- Pollen is confirmed as being a reliable, although imprecise (i.e., decadal time-scales) dating tool that can be applied in both estuarine muds and sands. The method requires an accurate catchment landcover history to be available. The method is simple and the key assumption that must be made relates to the time-lag for a pollen type to enter the stratigraphic record. Determining the pollen lag-time becomes of critical importance over decadal time scales

because the lag can be a substantial proportion of the time-scale of interest. Pine pollen is a particularly useful marker in Auckland estuarine sediments.

- ^{137}Cs (half-life = 30 yr), a product of atmospheric nuclear-weapons testing, is a reliable and precise dating method. The initial appearance of ^{137}Cs in the sediment column dates initial ^{137}Cs deposition (1953) in New Zealand. The main source of uncertainty is that ^{137}Cs may occur deeper in the core than can be detected. This uncertainty is minimised by increasing dry sample mass (~60 g) and counting time (24 hours) from previous work (Craggs et al. 2001). The close agreement between the initial introduction of ^{137}Cs in 1953 and the 1950 pine pollen layer in most of the cores provides a high degree of confidence in calculated SAR. However, ^{137}Cs will eventually disappear (i.e., within next 50 years or so) from the stratigraphic record due to radioactive decay.
- ^{210}Pb , a natural radioisotope (half-life = 22.3 yr), is potentially a reliable and precise dating tool, which can resolve short-term variations in SAR. The validity of ^{210}Pb dating rests on how accurately the ^{210}Pb delivery processes to the estuary are modelled. Exponential decay profiles fitted to the ^{210}Pb data were used to calculate SAR and particle residence time in surface mixed layers, where they occurred. An advantage of ^{210}Pb dating is that SAR are calculated from the entire profile rather than just the presence or absence of a tracer (e.g., ^{137}Cs). Time-series of annual changes in SAR were also reconstructed using a constrained constant-rate-of-supply (CRS) model for cores with good linear regression fits to the ^{210}Pb data and no evidence of surface mixing. These time-series indicate in some cases a “levelling off” in SAR and in other cases acceleration in sedimentation rates during the last 50 years. A key test of the validity of these detail sedimentation chronologies is to compare the mean atmospheric ^{210}Pb supply rate (P) estimated from cores and from direct measurements. The range of P values estimated from our cores (0.0030–0.0107 Bq cm⁻² yr⁻¹) showed (1) small between-core variations within estuaries and (2) compared favourably with the directly measured atmospheric ^{210}Pb flux (0.0059 Bq cm⁻² yr⁻¹) at Howick (June 2002–June 2003) given the ±30% (2 standard deviations) interannual variation in P measured at Hokitika. When ^{210}Pb is verified by independent dating as well as by comparison of P values, then reliable and detailed chronologies of sedimentation over the last ~150 years can be reconstructed from cores.
- Post-1950/1953 sedimentation rates in the middle–lower reaches of the studied estuaries (2.7–5.8+ mm yr⁻¹) are an order of magnitude higher than before catchment deforestation. There is not much difference in SAR measured in different estuary types and muddy estuaries do not necessarily infill more rapidly. Pollen and ^{137}Cs dating shows that average SAR on the intertidal flats (4.3–4.7 mm yr⁻¹) are significantly ($p = 0.975$) higher, by 0.8 mm yr⁻¹, than on the sub-tidal flats (3.5–3.9 mm yr⁻¹). Average intertidal (4.7 mm yr⁻¹) and subtidal (2.9 mm yr⁻¹) SAR derived from ^{210}Pb dating were not significantly different ($p = 0.975$) because of the larger variability in SAR values. Over the last 50 years, intertidal flats have

shoaled by ~0.5 m, the significance of which can be grasped by considering the fact that the average high-tide water depth in many Auckland estuaries is < 1m.

- At decadal (management) time scales, sediment infilling of Auckland estuaries will continue at several mm yr⁻¹. The effects of catchment sediment loads will be greatest in tidal creeks, at the catchment outlet. Even in largely intertidal estuaries, there is still no evidence that sedimentation rates are slowing down. Sedimentation rates in Auckland estuaries over the last 50 years are 2–3 times higher than the average rate of sea-level rise at Auckland (1.3 mm yr⁻¹) since the early 1900's. Thus, sea level rise has only partially reduced the rate of estuary aging, which has been accelerated by increased catchment sediment runoff.
- All estuaries follow similar evolutionary paths as they infill with sediment. Water areas and depths decrease over time and as a result hydrodynamic and sedimentological characteristics and biological communities change (Roy et al. 2001). The relative dominance of the fluvial system increases as estuaries mature and tidal volumes shrink. As estuaries age and infill, sedimentation rates may increase, even in the absence of catchment sediment load increases, because the available deposition areas reduce in size and will occur if the sediment trapping efficiency does not change. Thus, the longevity of an estuary depends on the original area and volume of the central mud basin (Roy et al. 2001), sediment supply rate and trapping efficiency. However, as Auckland estuaries age their trapping efficiency will decrease and consequently SAR will decline as more sediment is exported to adjacent coastal waters.
- Auckland estuaries are at different points along this evolutionary cycle. Waitemata harbour retains substantial sediment accommodation space in its central mud basin, while the tidal creeks fringing it have largely infilled. In the Mahurangi estuary, the large tidal creek above Hamiltons Landing has largely infilled and sediment has now partially infilled the central mud basin, so that the subtidal volume of this system is shrinking. The Wairoa estuary represents the end-member of the evolutionary cycle and has reached 'old age' before most Auckland estuaries primarily because of its relatively large catchment (~311 km²) and increased soil erosion following catchment deforestation. Our core data show that (1) post-1950 SAR in Wairoa Bay (3–6 mm yr⁻¹) and in Te Matuku Bay, Waiheke Island, (4–9 mm yr⁻¹) are as much as an order of magnitude higher than ~100 years ago and (2) suggest that the Wairoa estuary now exports sediment to the coastal environment, with the adverse impacts of fine catchment sediments transferred to neighbouring estuaries and inner Hauraki Gulf.

1. Introduction

1.1 Background

The Auckland region is currently home to about a million people and a doubling of the population is anticipated to occur during the next 50 years. Urban development increases water and sediment runoff during the earthworks phase, and contaminant loads increase as urban areas mature, which alters the composition and quantity of sediments deposited in estuaries (Williams, 1976; Douglas, 1985; Williamson, 1993; Morrissey et al. 2000; Swales et al. 2002). While some of this catchment sediment runoff is discharged to the sea, part of the sediment load is deposited in estuaries. Estuaries are particularly vulnerable to the effects of catchment landuse changes because of their close proximity to the sediment source and physical and biological processes that promote sedimentation. Auckland's numerous and varied estuaries are highly valued features of the coastal environment, and are variously impacted by land runoff.

In recent environmental impact assessments, the effects of catchment development on Auckland estuaries have been predicted using numerical models. For example, numerical modelling has been used to assess the risk of significant adverse effects on the benthic ecology of the Okura and Mahurangi estuaries, arising from increased catchment soil erosion, estuary suspended sediment concentrations and sedimentation associated with various scenarios of future catchment development. In the Mangemangeroa estuary (Howick), predicted annual sedimentation rates were verified with measurements of recent annual average sedimentation derived from caesium-137 (^{137}Cs) dating of cores. There was good agreement between measured and modelled data (see Fig. 13 in Oldman and Swales 1999). However, the credibility of modelling predictions is under close scrutiny as they underpin ARC opposition to contentious land development proposals. There is a need to strengthen and test the modelling predictions with evidence of both natural and human-induced effects in a wide range of estuarine systems and sub-environments. Such evidence will improve the general acceptance of the reliability of modelling predictions and increase our ability to plan effectively for the future and to minimise adverse effects.

There is also a relatively poor understanding of the widespread effects of catchment development in the Auckland region over the last 50 years or so on receiving estuaries. This period is of particular interest as it coincides with rapid urbanisation of many Auckland catchments. The present study thus provides a regional "snap shot"

of the recent physical effects of catchment development and resulting sediment runoff on Auckland estuaries.

Equally important, is the need to identify robust indicators that can be used to quantify the physical effects of catchment sediment runoff on estuaries. Hume et al. (2002) reviewed the relative merits of methods commonly used to reconstruct impacts of catchment development on estuaries based on analysis of sediment cores. In our field study, we have tested the utility of physical indicators identified in phase one by sampling sediments in a diverse range of estuary types and sub-environments.

Evidence for the effects of human activities on the quality and quantity of catchment sediment runoff is preserved in estuarine sediments. It is possible to obtain this evidence by coring estuarine sediments. In certain environments where sediments have accumulated undisturbed, the complete sequence and composition (or stratigraphic record) of sediment enables environmental changes in both the catchment and estuary to be reconstructed (e.g., Abraham and Parker, 2002; Swales et al. 2002). Where sediment deposits are remobilised, mixed or removed by waves and/or tidal currents, the stratigraphic record will be incomplete or completely erased. Also, even in quiescent depositional environments, biological mixing or bioturbation of sediments will also limit how accurately an estuary's past can be reconstructed, particularly if sedimentation is slow (Valette-Silver, 1993).

1.2 Limitations of present knowledge

The sedimentation effects of human activities in catchments have been reconstructed for several Auckland estuaries in the last twenty years or so, including the Upper Waitemata Harbour, Mahurangi, Pakuranga and Mangemangeroa (Hume and McGlone, 1986; Swales et al. 1997; Oldman and Swales, 1999; Swales et al. 2002). These studies have shown how catchment deforestation in the last 150 years, conversion to pasture, and in some cases urbanisation have permanently altered the quality and quantity of sediments deposited in receiving estuaries. Information provided by these studies is difficult to directly compare because the cores have been analysed in different ways. For example in the Mahurangi Study (Swales et al. 1997), pollen data were used to identify sediments deposited before and after catchment deforestation. The temporal resolution of the sediment dating was limited by the catchment history and in this example sediments deposited since 1900 represented the most recent historical period. By comparison, the additional sediment-dating methods used in the Pakuranga and Mangemangeroa studies (Oldman and Swales, 1999; Swales et al. 2002) enabled a more accurate and finely resolved record of estuary sedimentation patterns in the last 50 years to be constructed. Radioisotopes,

such as ^{137}Cs and lead-210 (^{210}Pb), were used to date recent sediments. The application of these methods to sedimentation studies does not rely on a detailed knowledge of catchment history. Our previous work also shows the critical importance of using several complimentary indicators to accurately quantify the effects of catchment soil erosion on estuarine sedimentation.

The limitations of our present knowledge of the effects of catchment development on sedimentation in Auckland estuaries relate to the relatively small number of estuaries that have been studied and the different methods adopted. A robust comparison of the effects of catchment sediment runoff on different estuary types and environments (e.g., intertidal versus subtidal) requires that a standardised methodology be adopted. The standard indicators that we have selected are ^{137}Cs , pollen, zinc (Zn) and particle size. The first appearance of ^{137}Cs in the environment coincides with the start of large-scale atmospheric nuclear weapons tests in the early-1950's (Matthews, 1989). Previous studies of Auckland estuaries have proven the value of pollen as a dating tool when the catchment history is well known. The concentration of heavy metals, such as zinc, is a useful indicator for identifying urban sediments. Zn concentrations in urban sediments are substantially higher than background concentrations in estuarine sediments (Williamson, 1993). Also, the increasing mud content of estuarine sediments has been shown in some cases to coincide with catchment development (Swales et al. 2002) as well as other large-scale environmental changes within the estuary, due to infilling or shifts in channel locations (Swales et al. 1997). We also evaluate ^{210}Pb data, which is also yielded by radioisotope analysis of sediments and provides an additional independent dating method.

1.3 Study objectives

The objectives of the phase-two field study are to:

- Re-construct a regional 'snap-shot' of the present physical condition and recent sedimentation history (i.e., last 50 years) of a representative cross-section of Auckland estuaries based on standard indicators.
- Provide empirical evidence documenting the effects of catchment soil erosion on a range of estuary habitats.
- Undertake a filling in of some of the knowledge gaps identified in the phase I literature review undertaken in 2000/01.

- Identify potential State-of-the-Environment physical indicators for estuaries.
- Provide empirical data to support numerical model predictions of estuary sedimentation associated with past (hindcast) and likely future (forecast) catchment development.
- Develop a conceptual physical model of how Auckland's estuarine systems will likely be impacted by future catchment sediment runoff.

2. Methods

2.1 Rationale

The phase-one literature review showed that previous studies of sedimentation in Auckland estuaries had largely focused on tidal-creek environments (Hume et al. 2002). Tidal creeks are usually narrow and funnel-shaped with shallow subtidal or intertidal channels with low-gradient intertidal mud flats often colonised by mangroves. Large compound estuaries, such as the Manukau, or drowned-valley estuaries, such as the Waitemata, are fringed by numerous tidal creeks. The focus on tidal creeks reflects the fact that tidal creek sediments usually preserve undisturbed stratigraphic sequences. This is because of their close proximity to the catchment outlet and sedimentation rates (e.g., $\sim 20 \text{ mm yr}^{-1}$, Swales et al. 2002) that may be an order of magnitude higher than the main body of the estuary, so that sediment-mixing processes, such as bioturbation, are less effective. Furthermore, the muddy tidal creek sediments accumulate radioisotopes, heavy metals and other contaminants, which are readily adsorbed by mud particles. However, tidal creeks represent only one sub-environment and usually a small fraction of the total estuary surface area.

To address the relative paucity of sedimentation data collected in the main body of Auckland estuaries our study focuses on the middle and lower reaches of estuarine systems. Furthermore, studies of relatively large estuarine systems, such as the Mahurangi, suggest that sedimentation patterns in middle–lower reaches of estuaries are spatially much more uniform than in tidal creeks (Swales et al. 1997). Consequently, we can have more confidence in conclusions drawn from analysis of cores collected in a particular sedimentary sub-environment. Also, importantly, the diversity of benthic macrofaunal communities is typically higher in the more sandy substrates and saline conditions found in the middle–lower reaches of estuaries than in the muddier substrates undergoing salinity gradients such as are found in tidal creeks (e.g., Hewitt et al. 1998, Norkko et al. 2001). Due both to their diversity and to their lower tolerance of fine sediment, benthic communities found in muddy-sand and sand substrates of the middle–lower reaches of estuaries are generally more adversely affected by fine-sediment runoff and subsequent increased water turbidity and deposition than tidal-creek fauna (Norkko et al. 2001).

Hume et al. (2002) define several common types of estuaries found in the Auckland region: drowned-valleys (e.g., Waitemata), tidal-lagoons (e.g., Puhoi), compound estuaries, and coastal embayments (e.g., Whitford). A representative selection of

estuary types is sampled in our study. Also, we selected estuaries with catchments at different stages of development, from mixed regenerating indigenous forest and pasture to estuaries with partly urbanised or urbanising catchments and where urbanisation or land-use intensification (i.e., life-style blocks) is likely to occur. Accordingly, several estuaries representative of the most common types were selected in consultation with the Regional Council (Fig. 2.1).

Drowned valley estuaries

- Waitemata (Te Atatu and Henderson cores)
- Mahurangi
- Okura
- Wairoa

Drowned valley estuaries are the most common estuary type in the Auckland region. Importantly, the selected estuaries cover the entire range of infilling stages. The Waitemata Harbour is partially infilled, but essentially remains largely subtidal. Infilling is most advanced in the tidal creeks of the upper Harbour. Infilling of the Mahurangi estuary is more advanced, with intertidal flats accounting for ~55% of its high tide area (Swales et al. 1997). Only in the lower reaches of the estuary do substantial subtidal areas remain. The Okura estuary has substantially infilled with sediment, with extensive intertidal flats flanking a narrow tidal channel. Mangroves are largely restricted to the tidal flats fringing the upper estuary. The Wairoa estuary (Clevedon) represents a mature drowned valley estuary, which has completely infilled with muddy sediments with extensive intertidal mangrove mud flats. Anecdotal evidence suggests that the Wairoa River is likely to export a large proportion of its sediment input to adjacent coastal waters. To confirm whether or not sediment discharged from the Wairoa is impacting the wider coastal environment, subtidal cores were also collected from the adjacent embayment between Whakakaiwhara and Pouto Points (Fig. 3.46).

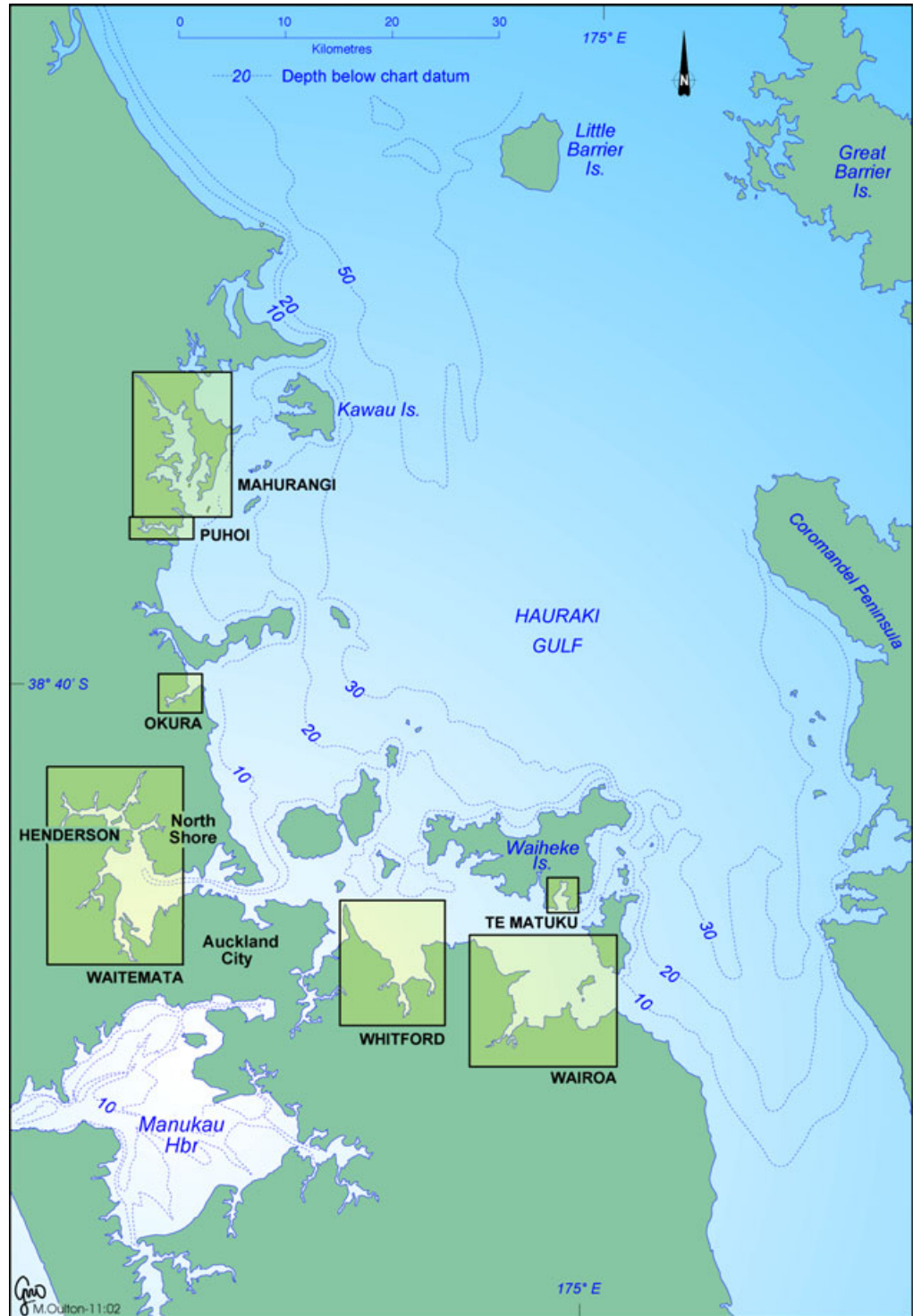


Figure 2.1: Auckland estuaries selected for the regional sedimentation study.

Tidal Lagoons

- Puhoi.

The Puhoi estuary is representative of several tidal lagoons that fringe Auckland's east coast, such as the Orewa, Waiwera and Whangateau (Omaha). Tidal lagoons form where barrier systems, usually Holocene sandy spits, have built across bays or the mouth of a drowned river valley to enclose a marine water body. Tidal lagoons are typically highly infilled and have extensive areas of intertidal sand flats cut by narrow drainage channels. Typically about 70% of the surface area is intertidal (Hume and Herdendorf 1992). As a consequence, flows in the main body of the estuary are dominated by the tides, and tidal pumping facilitates exchange and flushing between the estuary and the sea. Freshwater and sediment inflow is small for most of the time. Episodic floods dump mud in the narrow creeks in the headwaters. Mud is transported to the main body of the estuary but its fate is dependent on the timing of the tides and flood event. At low tide the channels act like rivers and transport suspended material seawards and mud can completely bypass the estuary by this mechanism. If the flood coincides with a rising and high tide, then mud is likely to be deposited on the sand flats. Sediments tend to be sandy in the middle and lower reaches of the main estuary, where wind-generated waves work to winnow mud from the sands. Ebb and flood tide shoals are built at the entrance from marine sands. The water in tidal lagoons has low turbidity for most of the time because a large proportion of the tidal prism¹ is exchanged with the open sea during each tide.

Coastal embayments

- Whitford Bay.
- Te Matuku (Waiheke Island).

A coastal embayment is an extension of the sea into a recess or indentation in the coast. Whitford Bay is a compound estuary and is best thought of as a series of tidal creeks draining to a coastal embayment. Coastal embayments lie on the open coast, and are common on offshore islands (e.g., Te Matuku). Coastal embayments generally have little freshwater input and catchment sediment runoff has little effect in these estuaries. However, in situations where runoff is greater, like at Whitford

¹ The amount of water that flows into an estuary on the incoming tide is termed the *tidal prism*. The outgoing tide comprises a larger amount of water than the flood tide because it contains river flow as well as tidal flow. The size of the tidal prism varies with the tidal range, with more water entering the estuary on a spring tide than on a neap.

where tidal creeks drain into the embayment, then catchment sediment runoff will result in greater sedimentation in the embayment. Whitford Bay (Fig. 2.1) is the focus of a jointly funded ARC, Manukau City Council and FRST study to assess the potential effects of sediment runoff, associated with future catchment development, on the benthic ecology. Data collected during this work has been used to assist selection of core sites. Furthermore, sedimentation rates derived from analysis of sediment cores will provide validation data for the sediment modelling. The Te Matuka embayment has largely infilled with muddy sediments and represents an end member coastal embayment (Fig. 2.1). This estuary receives runoff from a mixed pasture/native forest catchment.

Within each studied estuary, sediment cores were collected from depositional environments where relatively undisturbed sedimentation records were likely to be preserved. Muddy substrates occur in low wave-energy environments, where physical sediment mixing is less likely to occur, although biological mixing (i.e., bioturbation) may be more effective. Furthermore, radioisotopes and heavy metals, used to reconstruct recent estuarine sedimentation history, are preferentially associated with muds (i.e., particle diameter < 63 μm). To ensure that we can make valid comparisons between estuaries it is important to make comparisons between similar sedimentary environments. To satisfy these constraints, two sedimentary environments were selected:

- Intertidal muddy sandflats.
- Sub-tidal flats (< 10 m below chart datum (CD)).

To provide confidence in the sedimentation histories reconstructed from the sediment cores, we collected three replicate cores from discrete intertidal and subtidal flats within each studied estuary. This approach also allows us to test our hypothesis that sedimentation in the main body of estuaries is spatially more uniform than the tidal creeks where most previous sedimentation work has been undertaken.

2.2 Dating of recent estuarine sediments

Radioisotopes, such as caesium-137 (^{137}Cs) and lead-210 (^{210}Pb), and plant pollen can be used to reconstruct the sedimentation history of an estuary. Heavy metal (i.e., Pb, Zn and Cu) profiles in estuarine sediments have also been shown to provide useful additional information to identify the onset of urbanisation (e.g., Valette-Silver, 1993; Abraham and Parker, 2002; Swales et al. 2002). Complementary dating of estuarine sediments by independent methods offsets the limitations of any one approach. This

is particularly important given the confounding effects of physical and biological mixing when interpreting sediment profiles from lakes and estuaries (Robbins and Edgington, 1975; Olsen et al. 1981; Alexander et al. 1993; Valette-Silver, 1993; Benoit et al. 1999; Chagué-Goff et al. 2000).

Importantly, our measurements of recent sedimentation in Auckland estuaries substantially improve on the existing knowledge-base of (primarily) tidal creeks by:

- sampling the major intertidal and sub-tidal flat sub-environments in a wide variety of estuarine types, including drowned-valley, coastal embayments and tidal lagoons;
- sampling sub-environments in the relatively more ecologically diverse main body of estuaries;
- quantifying spatial variability in sedimentation rates at sub-environment scale by collecting and analysing replicate sediment cores;
- application of a standardised suite of complementary dating methods and physical indicators to determine the physical effects of catchment sediment runoff preserved in estuarine sediments.

2.2.1 Pollen dating

Historical landcover changes, such as catchment deforestation, establishment of pasture, plantation forestry or urbanisation alter the composition of the pollen assemblage. Pollen is delivered to estuaries by direct atmospheric deposition and in catchment runoff. Thus, changes in the abundances of plant pollen in estuarine sediments can be used for dating deposits if the history of catchment landcover change is known. The uncertainty in aging sediment cores using pollen largely depends on two factors: (1) the degree of *in situ* sediment mixing, the efficiency of which declines as sedimentation rate increase and (2) the time lag between the initial introduction of new plant species and production of sufficient pollen to be detectable in the stratigraphic record. The time lag for pollen production varies between plant species. New Zealand native trees take up to 50 years to reach full reproductive maturity whereas the introduced pine, *Pinus radiata*, develops a substantial pollen rain within 10 years. Grasses, weeds and other short-lived plants flower immediately and enter the stratigraphic record quickly. Swales et al. (2002) assumed a pollen dating uncertainty of ≤ 5 yr, based on the time lag for pollen production by exotic trees and grasses, which we adopt here. Therefore, the depth boundaries identified for post-

European (i.e., post-1850 AD) sediments may post-date the landcover change by ≤ 5 yr.

Pollen grains and spores (palynomorphs), are produced in huge numbers by conifers, flowering plants, ferns, and fern allies. Most palynomorphs are in the size range 5–120 μm , and thus can be easily transported by wind or water. In the presence of oxygen and moisture the cytoplasm decays rapidly, but the tough, decay-resistance outer wall tends to persist although it will eventually breakdown. If sediments are water-saturated, and thus oxygen levels are reduced to very low levels, the outer walls can persist indefinitely. A cubic centimetre of most soils and estuarine sediments will contain thousands of pollen grains and spores. Palynomorphs are most often identified to a familial or generic level, although a substantial number can be attributed to one or several closely related species.

There are three main pathways by which palynomorphs are incorporated into estuarine stratigraphic record:

- airborne palynomorphs may fall directly onto the surface of the estuary or the overlying water mass;
- palynomorphs drop directly onto the surface of catchment soils and waterways and are carried to the estuary;
- palynomorphs in catchment soils, rocks and other sediments are reworked (10^1 – 10^6 yr after initial deposition) and transported down stream networks and into the estuary.

The final palynomorph assemblage will always reflect varying proportions of these three pathways. Airborne palynomorph suffer no corrosion and little breakage before incorporation in sediments. Palynomorphs reworked along waterways will show some corrosion or breakage if they spend time in sediments along stream-banks and beds where bacteria are active. Soils, however, have a dramatic effect on palynomorphs. Fern spores are highly resistant to corrosion, but flowering plant pollen is highly susceptible and conifers have intermediate resistance to corrosion. The longer a collection of palynomorphs is in the soil, the more fern spores and, in particular, tree fern spores will dominate. A well-drained (aerated) soil will lose nearly all palynomorphs except for extensively corroded tree-fern spores. Thus, an estuarine sediment dominated by tree-fern spores is nearly always the result of a pollen source dominated by eroded catchment soils.

Major pollen assemblages and their interpretation

In the Auckland region, native conifers such as *Dacrydium cupressinum* (rimu), and *Prumnopitys taxifolia* (matai) made up the bulk of the forest pollen, but a range of broadleaf trees and shrubs such as *Weinmannia* (kamahi), *Alectryon excelsum* (titoki) are always present. These forests nearly totally covered the entire Auckland region before human settlement but now survive as scattered forest remnants. When the forest cover was complete, forest pollen did not dominate the estuarine palynomorph record because of the high input of tree fern spores, but native tree pollen did make up almost all of the non-spore total.

Bracken (*Pteridium esculentum*) spores are produced in large numbers, and are wind-dispersed and corrosion-resistant. Bracken and scrub covered most of the Auckland area after Maori settlement and forest clearance. While early European farming reduced the dense bracken stands of the Maori era, logging and burning continued to increase the catchment area where bracken was common. Bracken was a dominant landcover in the deforested Auckland catchments until the large-scale conversion to pasture from the late-1800's. This situation continued until the intensive farming and afforestation of the early 20th century. However, soils rich in bracken spores are common in some estuarine catchments and thus a steady influx of bracken spores continues even when bracken has been nearly eliminated from the local area (Wilmshurst et al. 1999).

Pine (*Pinus*) pollen is probably the most abundantly produced and widely distributed of all types (exotic and native) in the New Zealand flora. Slicks of yellow pollen that are particularly noticeable after rain on suburban streets are often derived from pine plantations many kilometres distant. Pine trees were planted from the beginning of European settlement in the mid-1800's, but had a relatively minor impact on the local and regional pollen rain. The first major plantations in the Auckland area were planted from the early 1930's at Woodhill, on the west coast, and Riverhead Forest in the Upper Waitemata Harbour catchment and smaller areas (e.g., Pukapuka Inlet, Mahurangi; Swales et al. 1997) were planted at about the same time. Elsewhere in the Auckland region, establishment of large-scale (i.e., 100–1000's ha) pine forests (*P. radiata* in particular) occurred from the mid-1970's in the Mahurangi, Puhoi, Okura and Hunua catchments.

Pine trees begin to flower as soon as five years after planting. However, pine pollen production depends on tree size and the distance pollen is dispersed is proportional to the height above the ground at which it is released. Pollen production from a pine plantation therefore gradually increases over time, reflecting the number of saplings

coming into flower (as all the trees are not planted at once), tree height and the foliage coverage. Pollen contributions from a plantation should first become apparent after 5 years, but the full effect is delayed until 10–15 years after planting. The net effect has been that, in areas remote from large plantations, there has been a general increase in the amount of pine pollen in estuarine sediments from the 1930s onward. In the Auckland region, the prevailing south-westerly wind would transport pine pollen east from Woodhill forest. However, because of the distance of Woodhill forest from the east coast estuaries as well as the 10–15 year time-lag between initial plantings and full pollen production, this contribution to the regional pollen rain was relatively slight in the 1930's–1940's. By 1950, with the first rotations of the Woodhill and Riverhead forests maturing, their consistent influence would be represented by a step-up of pine pollen percentages in estuarine sediments from trace or background levels to several percent. Continued plantings and expansions of existing forests would have consistently increased these levels through the 1960's. In the mid-1970's, the major increase in forest plantings that occurred in the Auckland region would have rapidly increased the regional pine pollen rain and by the early 1980's pine pollen levels in the environment and subsequently estuarine sediments would have approached those of the present day.

At the scale of individual catchments, the amount of pine pollen deposited in estuarine sediments depends greatly on whether or not there is pine forest in the catchment adjacent to the waterways. If there is, then pine pollen levels are higher than otherwise, and the effect of pine forest establishment is clearly evident in the estuarine sediments. In this situation, the gradual regional increase in pine pollen content from the 1930's abruptly increases after the mid-1970's with the establishment of local pine forests. Thus, in our study, the history of pine planting in the Auckland region is an important tool for dating estuarine sediments.

In interpreting the pine pollen signal in our cores, we assume a typical sigmoidal growth curve, in that after an initial period of rapid increase, the rate of pine growth declines and eventually plateaus as maturity is reached. This sigmoidal growth curve is mirrored in the pollen production, with an initial rapid increase, which eventually stabilises to roughly uniform level of year-to-year pollen production. This pattern is observed in many of the sediment cores collected for this study, firstly for the initial west coast forest planting in the 1930's and secondly following planting of *P. radiata* forests in several of the east coast estuary catchments (Fig. 2.2).

Grass (*Poaceae*) is now the predominant non-urban land cover, although lawns and verges within urban areas are also sources of grass pollen. However, grass pollen is not well represented in the estuarine samples, which likely reflects the large

reworked component of tree ferns and bracken, and the greater dispersal ability of pine pollen. Grass pollen does increase towards the present (top-most sediments) in most cores, paralleling the increase in pine pollen.

There are a large number of pollen types, which indicate either weedy pasture or road verges or urban settlement. Chief among these indicating weed communities are *Rumex* (dock/sorrel), *Plantago* (plantain), *Trifolium* (clover), and *Salix* (willow). *Acacia* and *Ligustrum* (privet) indicate more densely settled areas with hedgerows.

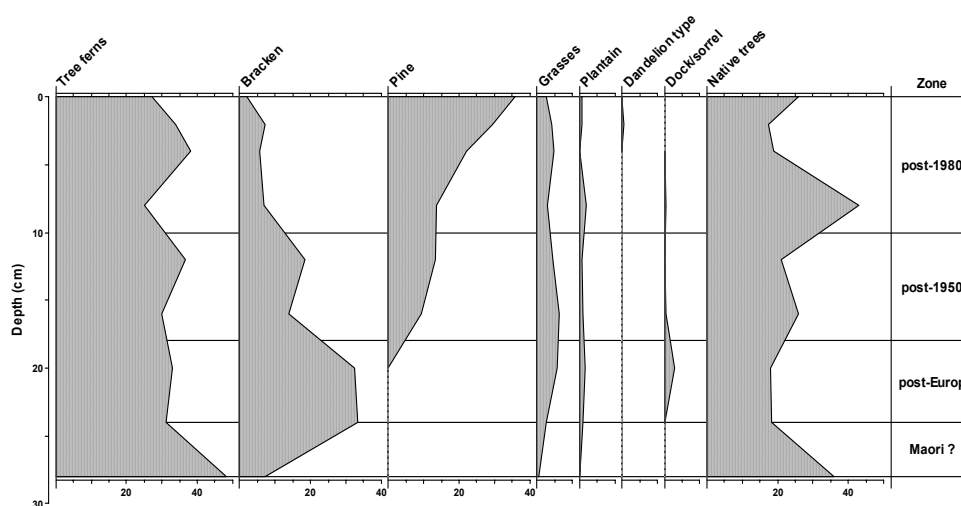


Figure 2.2: An example of pollen assemblage preserved in Te Matuku Bay (Waiheke Island) intertidal sediments (core TM-I1). Note the initial gradual rise in pine pollen, attributed to the initial planting of the Woodhill and Riverhead Forests (early 1930's), and subsequent rapid increase in pine pollen content, attributed to the planting of the Hunua Forest from the mid-1970's. The pollen and spore signal preserved in the Te Matuku Bay sediments is particularly clear, which is due to the inclusion of basal sediments that pre-date European settlement.

A number of families of wetland plants such as sedges (*Cyperaceae*) and jointed rushes (*Restionaceae*) are represented, but never in large quantities reflecting the dominance of input from catchment vegetation and reworked soils. *Avicennia* (mangrove) pollen is never common, and is rarely encountered even when mangrove covers the mudflats.

Historical zone definition

As many as five pollen assemblages, characteristic of discrete historical periods are identified in the sediment cores, which includes the original native forest and historical landcover changes since Maori settlement:

- *pre-Maori* (before 700 AD), characterised by high levels of native forest types with bracken and grass absent;
- *Maori* (700–1840±10 yr AD), characterised by high levels of bracken and native forest types in the absence of exotics;
- *post-European* (1840±10 yr–1950 AD): moderate to low levels of bracken, low levels of exotics with some grass;
- *post-1950* (1950–1980 AD): pine pollen content ≥5% of total palynomorphs. The ≥5% threshold reflects the minimum pine pollen content that can be reliably quantified and is indicative of the pollen rain that could be expected 5–15 yr after initial pine planting at Woodhill and Riverhead. Grass content is usually low with exotic trees, shrubs and weeds common;
- *post-1980* (post-1980 AD): pine content ≥10% of total palynomorphs. The ≥10% pine pollen threshold reflects the minimum increase that can be reliably quantified and is indicative of the pollen rain that could be expected 5–15 yr after initial planting of **local pine forests**. Grass content is high usually with reducing bracken and exotics common.

2.2.2 Radioisotope dating

^{137}Cs (half-life 30 yr) was introduced to the environment by atmospheric nuclear-weapons tests in 1953, 1955–1956 and 1963–1964. Peaks in annual ^{137}Cs deposition corresponding to these dates are the usual basis for dating sediments (Wise, 1977; Ritchie and McHenry, 1989). Although direct atmospheric deposition of ^{137}Cs into estuaries is likely to have occurred, ^{137}Cs is also incorporated into catchment soils, which are subsequently eroded and deposited in estuaries. In New Zealand, ^{137}Cs deposition was first detected in 1953 and its annual deposition was been measured at several locations until 1985. The annual ^{137}Cs deposition can be estimated from rainfall using known linear relationships between rainfall and Strontium-90 (^{90}Sr) and measured $^{137}\text{Cs}/^{90}\text{Sr}$ deposition ratios (Matthews, 1989). In Auckland, ^{137}Cs profiles

measured in estuarine sediments bear no relation to the record of annual ^{137}Cs deposition (i.e., 1955–1956 and 1963–1964 ^{137}Cs -deposition peaks absent), but rather preserve a record of catchment soil erosion. In our study, the maximum depth of ^{137}Cs occurrence in the sediment cores is taken to coincide with the year 1953, when ^{137}Cs deposition was first detected in New Zealand. We assume that there was no delay in initial atmospheric deposition of ^{137}Cs in estuarine sediments (e.g., ^{137}Cs scavenging by suspended particles) whereas there is likely to have been a small time-lag (i.e., < 1 yr) in ^{137}Cs inputs to estuaries from topsoil erosion, which would coincide with the occurrence of floods.

^{210}Pb (half-life 22.3 yr) is a naturally occurring radioisotope and has been widely applied to dating recent sedimentation (i.e., last 150 yrs) in lakes, estuaries and the sea. ^{210}Pb is an intermediate decay product in the uranium-238 decay series. The intermediate parent radioisotope radium-226 (^{226}Ra , half-life 1622 years) yields the inert gas radon-222 (^{222}Rn , half-life 3.83 days), which decays through several short-lived radioisotopes to produce ^{210}Pb . ^{226}Ra in estuarine sediments is supplied by catchment particulate inputs and ^{210}Pb derived from the *in situ* decay of ^{226}Ra is termed the supported ^{210}Pb (Oldfield and Appleby, 1984). A proportion of the ^{222}Rn gas diffuses from catchment soils into the atmosphere. Decay of ^{222}Rn in the atmosphere forms ^{210}Pb , which is deposited at the earth surface by dry deposition or with rainfall. Some of this atmospheric ^{210}Pb component is incorporated into catchment soils and is subsequently eroded and deposited in estuaries. Both the direct and indirect (i.e., soil inputs) atmospheric ^{210}Pb input to receiving environments, such as estuaries, is termed the unsupported ^{210}Pb .

The concentration profile of unsupported ^{210}Pb in sediments is the basis for ^{210}Pb dating. It is assumed that supported ^{210}Pb and ^{226}Ra concentrations are in equilibrium. The unsupported ^{210}Pb concentration is the component of the total ^{210}Pb concentration in excess of the supported ^{210}Pb value, which in turn is estimated from the ^{226}Ra assay. The validity of the ^{210}Pb dating rests on how accurately the ^{210}Pb delivery processes to the estuary are modelled, and in particular the rates of ^{210}Pb and sediment inputs (i.e., constant versus time variable).

In the Auckland region, large-scale catchment landcover changes over last 150 years, due to deforestation, conversion to pasture and, more recently, catchment urbanisation have resulted in substantial increases in catchment sediment loads. Consequently, sedimentation rates in receiving estuaries have also increased.

There are two possible models that can be applied to date ^{210}Pb profiles under varying sediment accumulation rates: (1) constant initial concentration (CIC) and (2) constant rate of supply (CRS) models.

The main assumption of the constant initial concentration (CIC) model is that sediments have a constant initial unsupported ^{210}Pb concentration (at the sediment-water interface), despite temporal variations in the net dry-mass sedimentation rate (Robbins, 1978). Since sediments have the same initial unsupported ^{210}Pb concentration (C_0), the value of C (Bq kg^{-2}) will decline exponentially with age (t):

$$C_t = C_0 e^{-kt} \quad \text{Eq. 1}$$

where k is the radioactive decay constant for ^{210}Pb (0.03114 yr^{-1}), C_0 is the unsupported ^{210}Pb concentration (Bq kg^{-2}) at time zero, which in the absence of surface mixing will coincide with the sediment-water interface. The CIC model is feasible when the main source of unsupported ^{210}Pb is from eroded catchment soils. Furthermore, in environments where the water residence time is low, changes in the sediment flux would affect ^{210}Pb retention in sediments (Blais et al. 1995).

Using the CIC model, the age of sediments at depth x is given by:

$$t = \frac{1}{k} \ln \frac{C_0}{C} \quad \text{Eq. 2}$$

The CRS model assumes that there is a constant rate of supply of unsupported ^{210}Pb from the atmosphere to the lake or estuary waters and hence a constant rate of ^{210}Pb supply to the sediments despite variations in the dry-mass sedimentation rate (Goldberg, 1963). Furthermore, the assumptions of the CRS model are satisfied where the total cumulative excess ^{210}Pb in sediment cores collected at different sites, in the same sedimentary environment (e.g., a sub-tidal flat), are similar. In lake systems, the CRS model has generally been favoured over the CIC model because the main source of unsupported ^{210}Pb is believed to be direct atmospheric deposition and the water residence time is long compared to the particle settling time (e.g., Blais et al. 1995).

Using the CRS model, the age of sediments at depth x is given by:

$$t = \frac{1}{k} \ln \frac{A(o)}{A} \quad \text{Eq. 3}$$

where $A(o)$ is the total unsupported ^{210}Pb in the sediment column (Bq cm^{-2}) and A is the cumulative unsupported ^{210}Pb below sediments of depth x . The parameters A and $A(o)$ are estimated by integration of the unsupported ^{210}Pb profile and expressed as Bq cm^{-2} to correct for depth variations in sediment dry bulk density.

A more reliable sedimentation history can be established by constraining the CRS depth-age curve to pass through a sediment layer of age t_0 that has been independently dated. Furthermore, because the unsupported ^{210}Pb concentration decays exponentially with depth, an objective method is required to determine the depth of sediment over which to integrate the unsupported ^{210}Pb profile and thereby estimate $A(o)$ and A . We use the maximum depth of ^{137}Cs ($^{137}\text{Cs}_{\text{max}}$) to constrain the CRS model by calculating the residual unsupported ^{210}Pb in the sediment column below this sediment layer (A_{res}):

$$A_{\text{res}} = \frac{\Delta A}{e^{kt_0} - 1} \quad \text{Eq. 4}$$

where ΔA is the integrated unsupported ^{210}Pb in the sediment column above the dated sediment layer, e is 2.7182818..., k is the decay constant for ^{210}Pb and t_0 is the age of the sediment layer (49 years). The total unsupported ^{210}Pb in the sediment column, $A(o)$ used in Eq. 3 is then given by:

$$A(o) = \Delta A + A_{\text{res}} \quad \text{Eq. 5}$$

Uncertainty in $^{137}\text{Cs}_{\text{max}}$ results from the 4-cm depth interval between samples as well as the minimum ^{137}Cs concentration that can be detected, which is primarily determined by sample size and counting time. To determine the sensitivity of the CRS model to changes in $^{137}\text{Cs}_{\text{max}}$, we calculated $A(o)$ for three values of $^{137}\text{Cs}_{\text{max}}$:

1. Maximum depth at which ^{137}Cs detected in the core;
2. Depth of the next sample below (1)
3. Mid-depth between (1) and (2).

A dry bulk density (ρ_d) profile was constructed at 0.1-cm intervals to match the unsupported ^{210}Pb to the maximum depth determined by Eq. 5, from which the areal ^{210}Pb activity (Bq cm^{-2}) and hence $A(o)$ and A could be determined as follows. Within the top 29 cm of the sediment column we interpolated ρ_d from measured values. Below 29-cm depth we estimated ρ_d from linear regression of measured ρ_d values.

The mean annual flux (P) of unsupported ^{210}Pb to the sediment column can be estimated from $A(o)$ by:

$$P = kA(o) \quad \text{Eq. 5}$$

Comparing P to direct measurements of the mean atmospheric flux of ^{210}Pb is a useful test of the validity of the ^{210}Pb chronology determined for a particular site. Global atmospheric fluxes of ^{210}Pb are $0.0074\text{--}0.037 \text{ Bq cm}^{-1} \text{ yr}^{-1}$ (Oldfield and Appleby, 1984). In New Zealand, the mean annual atmospheric ^{210}Pb flux of 0.0117 (range: $0.0086\text{--}0.0136$) $\text{Bq cm}^{-2} \text{ yr}^{-1}$ measured at Hokitika during 1995–2000 is within the range of global values (Tinker and Pilvio, 2000). The mean annual atmospheric ^{210}Pb flux at Auckland is likely to be less than at Hokitika due to the substantially lower annual rainfall. We measured the ^{210}Pb concentrations in rainwater samples collected at monthly intervals during June 2002–June 2003 in the Mangemangeroa catchment (Topo Map 260 R11, 8250E 7220N) as part of NIWA's FRST-funded 'Effects of Sediments on Estuarine and Coastal Ecosystems'.



Figure 2.3: Mangemangeroa (Howick) rainfall station (Map 260 R11, 8250E 7220N). The rainfall sampler for ^{210}Pb deposition measurements (left) is serviced at monthly intervals. An automatic tipping bucket (front right) rain gauge provides rainfall intensity-duration data.

The measured ^{210}Pb flux for the June 2002–June 2003 period was $0.0059 \text{ Bq cm}^{-2} \text{ yr}^{-1}$. We use this measured value of P at Mangemangeroa as a guide to validate our ^{210}Pb dating.

Oldfield and Appleby (1984) provide guidelines to select the most appropriate ^{210}Pb dating model. In our study, both the CIC and CRS dating models may be applicable, depending on the depositional environment. For example, at sites close to catchment sediment sources (e.g., Henderson creek) the primary excess ^{210}Pb source is likely to be due to catchment soil inputs. Also, small estuaries and tidal creeks are largely intertidal and therefore the residence time of the estuarine water body is low (i.e., one tidal cycle) in comparison to most lakes (10–100's yr). Thus, under these conditions the CIC model is likely to be applicable. Direct atmospheric ^{210}Pb deposition is likely to be more important in large sub-tidal basins (e.g., middle Waitemata harbour) or in sheltered coastal waters (e.g., Tamaki Strait) because of their large surface areas, distance from catchment sediment sources and relatively long residence times compared to intertidal flats. In these environments we would anticipate that the CRS model would likely be more applicable. Both the CIC and CRS models are used to date the sediment cores.

Sediment Mixing

The CRS and CIC dating models were first applied to lake sedimentation studies and in their simplest form can be used to derive depth-age curves in the absence of substantial sediment mixing. In the case of the CRS model, where the surface mixed layer (SML) is less than ~15% of the total depth of the unsupported ^{210}Pb profile then the effect of mixing on age estimates is negligible (Oldfield and Appleby, 1984). In shallow estuaries, where sediment mixing by physical and biological processes can be intense, these models cannot be readily applied without taking into account mixing processes. Various mathematical models have been proposed to take into account the effects of bioturbation on ^{210}Pb concentration profiles (e.g., Guinasso and Schink, 1975). Biological mixing has been modelled as a one-dimensional particle-diffusion process (Goldberg and Kiede, 1962) and this approach is based on the assumption that the sum effect of 'random' biological mixing is integrated over time. In estuarine sediments exposed to bioturbation, the depth profile of unsupported ^{210}Pb typically shows a two-layer form, with a surface layer of constant ^{210}Pb concentration overlying a zone of exponential decrease (Fig. 2.4). However, to apply these types of models requires the assumption that the mixing intensity (i.e., Diffusion coefficient) and mixing depth (i.e., surface-mixed layer, SML) are uniform in time. The validity of this assumption cannot be tested, but changes in bioturbation process could be expected to follow changes in benthic community composition.

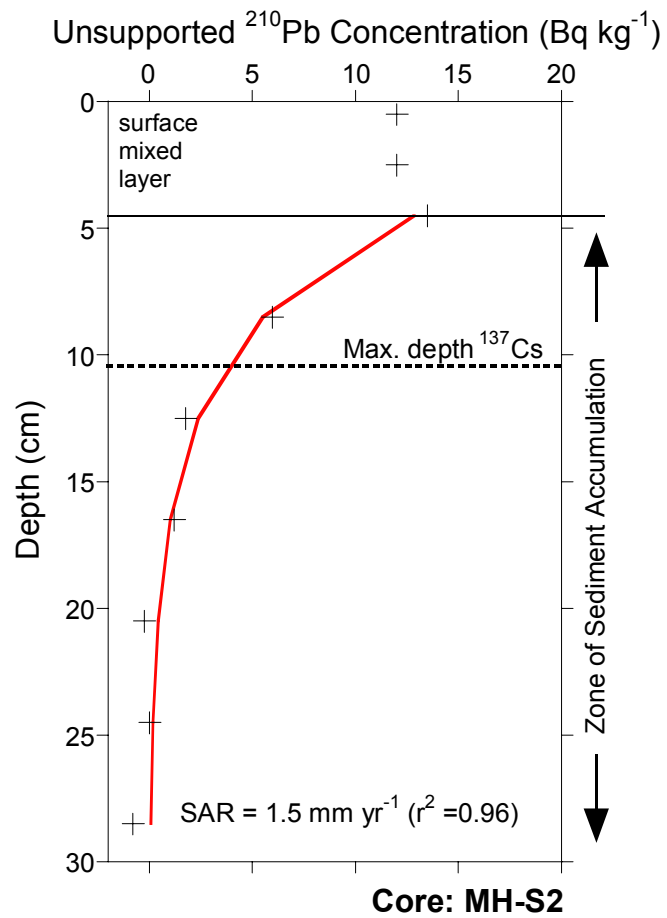


Figure 2.4: Effect of bioturbation on the depth profile of unsupported ^{210}Pb concentration at Mahurangi estuary subtidal core site MH-S2. The sediment accumulation rate (SAR) is calculated for the accumulation zone below the SML. Maximum ^{137}Cs depth at ~ 10.5 cm. Note that ^{210}Pb profiles are normally plotted on a log-scale. We use a linear scale here to illustrate the exponential decay behaviour.

Consequently, we only apply the CRS and CIC dating models where:

- SML <15% of the measured ^{210}Pb concentration profile depth;
- no other evidence (e.g., pollen profiles) suggests substantial mixing;
- a high coefficient of determination (r^2) for the linear regression models fitted to the natural-log transformed ^{210}Pb concentration profiles.

2.3 Sedimentation rates

Changes in sedimentation rates in estuaries provide by far the strongest evidence for the effects of catchment sediment runoff on estuarine systems.

Sedimentation rates are measured by calculating the thickness of sediment between dated layers in cores. The layers are dated ideally using complimentary methods as previously discussed in this report. Sedimentation rates calculated from cores are *net average sediment accumulation rates (SAR)*, which are usually expressed as **mm yr⁻¹**. These SAR are net values because cores integrate the effects of all the processes, which influence sedimentation at a given location usually over years, decades or centuries. However, at short time-scales (i.e., seconds–months), sediment may be deposited and then subsequently re-suspended. Thus, over the long-term, sedimentation rates derived from cores represent net or cumulative effect of potentially many cycles of sediment deposition and re-suspension. However, in practice, reliable records of historical sedimentation are usually only found in depositional environments where sediment mixing due to physical processes (e.g., re-suspension) and bioturbation is limited. The effects of bioturbation reduce as SAR's increase (Valette-Silver, 1993).

Net sedimentation rates statistics also mask the fact that estuary sedimentation is an episodic process, which largely occurs during catchment floods, rather than the continuous gradual process that is implied. For example, a single flood in May 1985 delivered 75% of the 20-year annual average sediment load to the Mahurangi estuary (Swales et al. 1997).

Although sedimentation rates are usually expressed as a sediment thickness deposited per unit time (i.e., mm yr⁻¹) this statistic does not account for changes in dry sediment mass with depth in the sediment column due to compaction. Typically, sediment density ($\rho = \text{g cm}^{-3}$) increases with depth and therefore some workers prefer to calculate dry mass accumulation rates per unit area per unit time ($\text{g cm}^{-3} \text{ yr}^{-1}$). These data can be used to estimate the total mass of sedimentation in an estuary (tonnes/yr) (e.g., Swales et al. 1997). However, in our experience of estuarine cores (up to 4 m long) the effects of compaction are often offset by changes in bulk sediment density reflecting layering of low-density muds (i.e., dry density $<1 \text{ g cm}^{-3}$) and high-density (i.e., dry density, $\rho_d, >1 \text{ g cm}^{-3}$) sand deposits. In the present study, the 0.3-m short cores, sediments are relatively homogeneous and the mass of overlying sediment insufficient to cause significant compaction. Furthermore, the significance of a SAR expressed as mm yr⁻¹ is more readily grasped than a dry-mass

sedimentation rate. For example, the rate of estuary aging (mm yr⁻¹) can be directly compared with the potential mitigating effect of sea level rise (mm yr⁻¹).

SAR from ²¹⁰Pb dating

In our study, we calculate a sediment accumulation rate for the zone of exponential ²¹⁰Pb concentration decrease. In some cases surface mixing is absent but typically a SML 2.5–12.5 cm thick is apparent from the ²¹⁰Pb profiles. The rate of ²¹⁰Pb concentration decrease with depth can be used to calculate a net sediment accumulation rate. Assuming that within a finite time period, sedimentation (S) or SAR is constant then $t = z/S$ can be substituted into Eq. 1 and by re-arrangement:

$$\frac{\ln\left[\frac{C_t}{C_0}\right]}{z} = -k/S \quad \text{Eq. 6}$$

For an exponential decay model, a depth profile of $\ln(C)$ should yield a straight line of slope $b = -k/S$. We fitted a linear regression model to natural-log transformed ²¹⁰Pb concentration data to calculate b . The sedimentation rate over the depth of the fitted data is given by:

$$S = -(k)/b \quad \text{Eq. 7}$$

An advantage of this method is that the sedimentation rate is based on the entire ²¹⁰Pb profile rather than a single layer, as is the case for ¹³⁷Cs. Furthermore, if the pollen or ¹³⁷Cs tracer is present at the bottom of the core then the estimated SAR is only a minimum value. The SAR found by the ²¹⁰Pb method can also be used to estimate the residence time (R) of sediment particles in the SML before they are removed by burial. For example, for core MH-S2 (Fig 2.4), R is given by the SML depth (45 mm) divided by S (1.5mm yr⁻¹) = 30 yr. Although this greatly simplifies the process (i.e., the likelihood of particle mixing reduces with depth in the SML), this approach provides a useful first-order estimate of R and the relative importance of sediment mixing between cores, sub-environments and estuaries.

Time-series of historical changes in annual sedimentation rates are also reconstructed for cores using the constrained CRS ²¹⁰Pb dating model where evidence of surface mixing is absent, with good linear-regression models fits to the natural-log transform ²¹⁰Pb profiles and good agreement with pollen and ¹³⁷Cs dating. In these cores, dry-mass annual sedimentation rates (S_{mass}):

$$S_{\text{mass}} = \frac{kA}{C} \quad \text{Eq. 8}$$

where S_{mass} is measured as the dry mass accumulation rate per unit area per year ($\text{g cm}^{-2} \text{ yr}^{-1}$), which can be converted to an annual SAR (mm yr^{-1}) using the dry bulk sediment density ($\rho_d = \text{g cm}^{-3}$):

$$\text{SAR} = \left(\frac{S}{\rho_d} \right) 10 \quad \text{Eq. 9}$$

SAR from pollen and ^{137}Cs dating

Average SAR were also estimated for three time periods using the pollen and ^{137}Cs data for three dated depth horizons:

- **1950 A.D.**, based on the rise in *P. radiata* pollen content to $\geq 5\%$ of the total pollen and spore count per sample;
- **1953 A.D.**, based on the maximum depth of ^{137}Cs in the sediment column;
- **1980 A.D.**, based on the rise in *P. radiata* pollen content to $>10\%$ of the total pollen and spore count, with high grass pollen and declining bracken content. Exotic trees and weeds common.

SAR were calculated for the time periods:

- **1950–1980 A.D.**, based on pollen profiles;
- **1980–2001 A.D.**, based on pollen profiles;
- **post-1950/1953 A.D.**, based on pollen/ ^{137}Cs profiles;

The pollen-dated 1950–1980 and 1980–2001 sediment layers provide information about how SAR may have changed during the last 50 years. The 1950 pollen and 1953 ^{137}Cs sediment layers enable SAR calculated by both dating methods for similar time-periods to be compared. In most of our cores *P. radiata* pollen is present in the bottom-most sample at 28.5-cm depth. This indicates that our cores post-date the

mid-1930's when pine pollen would have begun to appear in estuarine sediments from the Woodhill and Riverhead forests.

The presence or absence of pine pollen in the bottom-most sediment sample (28–29 cm depth) also provides additional information to validate the ^{210}Pb dating. Planting of the Riverhead and Woodhill forests occurred from 1927 and was largely completed by the early-1930's. The first appearance of pine pollen in the cores would be expected 5–15 yr after initial pine planting. Thus, the maximum age of sediments containing pine pollen is 60–70 yr (1942–1932 A.D.). Bioturbation, in particular, can potentially mix pollen down through the sediment column, however there are usually tell-tail signs in the profiles that we can identify, such as isolated spikes of pine pollen deep in cores (e.g., Okura core OK-I1 and Waitemata core WT-S3).

2.4 Sediment coring

Sediment short cores (i.e., 30-cm-long) were collected from the studied estuaries between October 2001 and January 2002. In total 30 cores were collected for sediment dating. A further 12 cores were randomly sampled (at the same time) within a 10-m radius of each sediment-dating core, for characterisation of the benthic macro-fauna in phase three (2002–2003) of this study. Relatively large-diameter (i.e., 10 cm internal diameter) cores were collected so that sufficient sediment mass was contained within 1-cm-thick sediment slices for radioisotope analysis. Intertidal sediment cores were sampled at low tide and SCUBA divers collected the sub-tidal cores. The PVC plastic core barrels were driven into the substrate using a sledgehammer and specially designed steel end cap to minimise disturbance of surface sediments. Compression of the sediments was negligible. The location of each primary (i.e., dating) core was fixed to ± 1 m (sub-tidal sites) using differential global positioning (DGPS) and to ± 10 –100 m for intertidal cores using a less accurate hand-held GPS (Appendix I).

2.5 Laboratory analyses

In the laboratory, the cores were split and 1-cm-thick slices sub-sampled at 4 cm depth intervals. An additional sub-sample was collected at 2–3 cm depth to improve estimates of the near-surface radioisotope concentrations in each core. Typically, a large proportion of the unsupported ^{210}Pb occurs in the top-most 10 cm of the sediment column. A 39 cm³ half-slice was taken to provide a nominal ~60 g of dry sediment for radioisotope analysis. In the Waiokopua estuary (Whitford) nominal 13 g sediment samples were used for ^{210}Pb dating (Craggs et al. 2001). However, the large uncertainties in the unsupported ^{210}Pb estimates precluded dating sediments by this

method. Because the primary source of uncertainty in the ^{210}Pb dating relates to the counting statistics, in the present study this uncertainty was minimised as far as possible by increasing sample size to ~60 g, which is the maximum amount that can be embedded in epoxy resin. Samples were weighed, dried at 105°C for 24 hours, re-weighed after 30 minutes cooling and ground to a coarse powder. The wet and dry weights of the samples were used to calculate wet and dry bulk sediment densities (g cm^{-3}) and water contents. The remaining half-slice of each sample was homogenised and 1 cm^3 taken for particle size analysis, with the remaining bulk of the half slice used for chemical analysis of Zn concentration.

Particle size was determined using a Galai CIS-100 'time-of-transition' (TOT) stream-scanning laser particle sizer operated by NIWA. Sediment sub-samples (~1 cm^3) taken from each 1-cm slice were wet-sieved through a 2mm sieve to remove leaf and twig fragments and shell hash. Sediment samples were dispersed by ultra-sonic dispersion for four minutes before and during particle size analysis. Typically 10^5 – 10^6 particles were counted per sample. Particle volumes, for spheres, were calculated from the measured particle diameters, which were used to determine the particle-size volume distribution for each sample.

Zinc concentrations were determined on 1 to 4 g of wet sediment in a 50 ml polypropylene centrifuge tube. A separate aliquot was dried overnight at 105°C for dry matter determination. To each tube 40 ml of 2M HCl was added to extract the reactive fraction of metals and the tubes were placed on a shaking table at 100 rpm for 24 hours. Samples were centrifuged at 3000 rpm for 15 minutes and the supernatant was decanted into new tubes for storage and analysis. Zinc was analysed by atomic absorption spectrometry using flame atomisation (Perkin Elmer 3110). Concentrations were corrected to dry weight and expressed as $\mu\text{g g}^{-1}$. Precision of the analyses was within 10%. A conservative estimate of the accuracy of the Zn concentrations is $\pm 5 \mu\text{g g}^{-1}$. Calculations were based on freshly prepared matrix matched working standards prepared from commercially available stock solutions.

Sediment samples (2–3 cm^3) for pollen analysis were prepared as described by Moore and Webb (1978). Following acid digestion, resistant minerals, pollen and spores were mounted on glass slides. Between 100–200 pollen grains and spores of terrestrial plants (i.e., all species combined) were counted on regular transects across each slide. The results are presented as percentages of a palynomorph sum including all types. Two sets of palynomorph diagrams are presented here: (1) major types with common names are used as summary diagrams and (2) more detailed diagrams with scientific names and all types included are presented in Appendix II.

Concentrations of the radioisotopes ^{226}Ra , ^{210}Pb and ^{137}Cs in sediment samples were analysed by the National Radiation Laboratory. Radioisotope concentrations were determined by high resolution, low-level gamma ray spectrometry using a Canberra Model GX6020 60% extended range germanium hyper-pure planar gamma detector. Samples were counted for 24 hours to minimise uncertainties in radioisotope concentrations. The ^{226}Ra concentrations of the sediment samples were determined from the emissions of the short-lived ^{222}Rn gas by embedding samples in epoxy resin. An “ingrowth” period of 30 days allows equilibrium to be reached between ^{222}Rn and its short-lived daughters ^{214}Pb and Bismuth-214 (^{214}Bi). Gamma spectra of ^{226}Ra , ^{210}Pb and ^{137}Cs were analysed using Genie2000 software (ver. 1.3). Radioisotope concentrations are expressed in S.I. units as becquerel (disintegration s^{-1}) per kilogram (Bq kg^{-1}). Depth profiles of ^{226}Ra concentration (Bq kg^{-1}) are presented in Appendix III.

The uncertainty ($U_{2\sigma}$) of the unsupported ^{210}Pb concentrations is given by:

$$U_{2\sigma} = \sqrt{({}^{210}\text{Pb}_{2\sigma})^2 + ({}^{226}\text{Ra}_{2\sigma})^2} \quad \text{Eq. 10}$$

where ${}^{210}\text{Pb}_{2\sigma}$ and ${}^{226}\text{Ra}_{2\sigma}$ are the two standard deviation uncertainties in the total ^{210}Pb and ^{226}Ra concentrations at the 95% confidence level. The primary source of uncertainty in the measurement of radioisotope concentrations relates to the counting statistics (i.e., variability in the rate of radioactive decay). This source of uncertainty can be reduced by increasing the sample size. The $U_{2\sigma}$ values in our cores were in the range 3.6–7.2 Bq kg^{-1} .

For sediment dating, we estimated ^{210}Pb concentrations at regular 0.1-cm depth increments from the linear regression of the natural-log transformed ^{210}Pb data. In cases where the ^{226}Ra concentration was higher than the total ^{210}Pb concentration (i.e., supported and unsupported ^{210}Pb) we assumed that unsupported ^{210}Pb was absent in that particular sample and excluded from the regression analysis. The unsupported ^{210}Pb profile for each core was calculated, using the fitted regression relation, from the surface to a maximum depth based on Equations 4 and 5. Figure 2.5 shows an example of a linear regression fit to the ^{210}Pb profile measured in core TM-I1 (Te Matuku - Intertidal Core One). It can be seen that the decline in unsupported ^{210}Pb concentration with depth in the sediment column is well described by the regression equation ($r^2=0.96$). In this example, the maximum depth for integrating the ^{210}Pb profile to determine $A(d)$ is 80 cm. The coefficient of determination (r^2) for the linear regressions fitted to the sub-tidal and intertidal cores varied between 0.65–0.96 and 0.20–0.96 respectively.

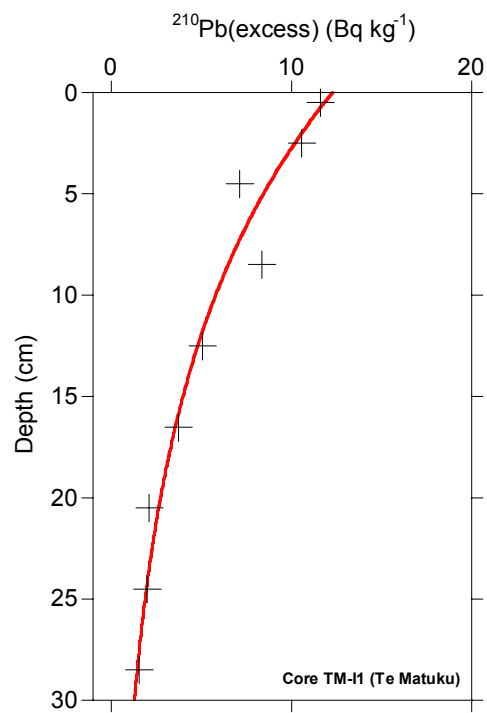


Figure 2.5: Example of log-linear regression fit ($r^2 = 0.96$) for excess ^{210}Pb concentration profile measured in core TM-11, Te Matuku Bay (Waiheke Island). $C \sim 0.05C(0)$ occurs at 40-cm depth.

3. Results

3.1 Estuary and catchment characteristics

Table 3.1 summarises key physical attributes of the studied estuaries. The estuaries vary in size and degree of infilling, as expressed by the proportion of intertidal area. Differences in the ratio of catchment to estuary (CER) areas indicates the capacity of an estuary to accumulate sediment runoff. The estuary high tide area is a surrogate measure for the original estuary basin volume. For example, the CER for the largely sub-tidal Waitemata and Mahurangi estuaries is 5 (i.e., catchment = 5 times estuary area). By comparison, the CER for the Wairoa estuary (~124) is an order of magnitude higher than for the Waitemata, which may explain why the estuary has reached an advanced state of infilling much earlier than the Waitemata and Mahurangi estuaries.

Table 3.1: Estuary and catchment characteristics (source: NIWA Estuary Environment Classification Database).

Estuary	Area (km ²)	Intertidal Area (%)	Mangrove Area (%)	Tidal Prism ¹ (10 ⁶ m ³)	Catchment Area (km ²)	Rainfall ² (mm yr ⁻¹)	CER ³
Mahurangi	24.6	51	20	44.9	122.2	1620	5
Okura	1.4	79	14	2.1	22.7	1320	16
Puhoi	1.7	71	27	2.7	43.0	1320	25
Henderson	2.0	–	–	–	105.1	1390	53
Waitemata	79.9	36	12	216.1	427.3	1390	5
Whitford	11.1	82	11	18.5	61.0	1180	6
Wairoa	2.5	42	42	5.2	311.2	1360	124
Te Matuku	2.0	76	19	4.4	12.2	1360?	6

Notes: (1) tidal prism estimated from the average surface area of estuary and spring tidal range. (2) rainfall is the areally weighted rainfall value obtained by overlaying the catchment boundary on the 30 year (1951-1980) normal rainfall map surface. (3) CER = Catchment/ Estuary (area) Ratio.

The estuaries included in our study fall into two groups: (1) estuarine systems with small CER (5–6) and (2) estuarine systems with large CER (16–124). Group one includes estuaries, which retain substantial sub-tidal areas (Mahurangi, Waitemata, Whitford), although Te Matuku is an exception. Group two is represented by the largely intertidal Puhoi, Okura, Henderson and Wairoa estuaries.

3.2 Mahurangi estuary (intertidal and sub-tidal cores)

3.2.1 Background

The Mahurangi estuary is one of the largest drowned-valley systems on Auckland's east coast (Fig. 3.1). The estuary has a high-tide surface area of 24.7 km² and a tidal volume of ~44.9 million m³ (Table 3.1). At low tide, the main tidal channel is flanked by extensive intertidal flats composed of sands and muddy-sands, which are fringed by extensive mangrove stands (Swales et al. 1997). The estuary receives runoff from a 122-km² catchment, of which 65% drains to the head of the estuary at Warkworth. The estuary is an important recreational resource, widely used for boating and fishing and is also the site of a large-scale (~120 ha) pacific oyster industry established in the early 1970's.

Catchment landcover originally consisted of undisturbed, mixed conifer-hardwood forest dominated by rimu, kahikatea, totara, matai, miro, hard beech, tree ferns and kauri (McGlone 1994). Sediment cores collected in the estuary by Swales et al. (1997) indicate that the activities of Maori had little effect on catchment landcover and sediment loads. Large-scale catchment deforestation occurred between 1840 and the 1880's (Harris, 1993). Initially, forests in sub-catchments draining to the lower estuary were logged and as these forests were depleted, logging activities moved progressively towards the head of the estuary. Much of the milled timber was used in ship construction at Te Kapa Inlet and Dyers Creek (Johnston, 1984). By the late 1800's only small forest remnants remained. At about this time, large-scale clearance of regenerating scrub for farming began, which involved scrub burnoff followed by planting of exotic grasses. By the early 1900's pastoral farming, orcharding and cropping were the predominant catchment land uses. Large-scale production forestry (mainly *Pinus radiata*) was established from 1975 and occupies the upper reaches of the Mahurangi River catchment (right branch). Logging of the first rotation began in 1997. The urban centres of Warkworth and Snells Beach represent a small fraction of the total catchment area.

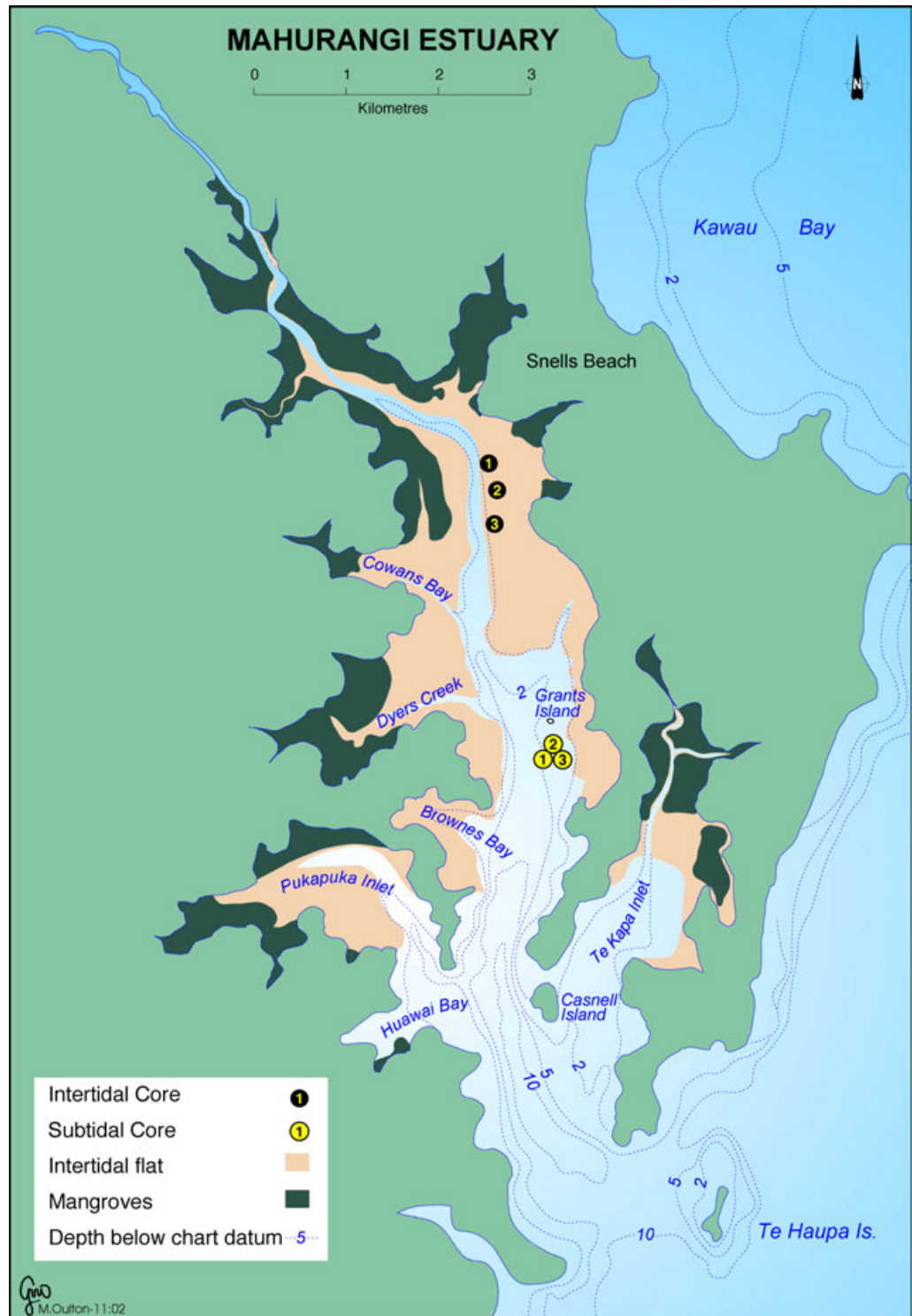


Figure 3.1: Mahurangi estuary - location of intertidal and sub-tidal cores and major sub-environments.

3.2.2 Mahurangi estuary sediments

Replicate sediment cores were collected from both intertidal and sub-tidal flat environments in the Mahurangi estuary (Fig. 3.1). Cores were taken from the extensive intertidal flats on the eastern flank of the main tidal channel north of Grants Island and from a subtidal flat ~0.5 km south of Grants Island between 4–5 m below chart datum. Both the intertidal and sub-tidal sediments were typically muddy fine-sands composed of fine silt (~20 μm modal diameter) and very fine sand (~100–150 μm modal diameter) (Fig. 3.2). The sub-tidal sediments also contained quantities of coarse sand-sized shell fragments. Dry bulk sediment densities in the cores vary between 0.75–1.5 g cm^{-3} with no clear trend of increasing density with depth in the sediment column (Appendix IV).

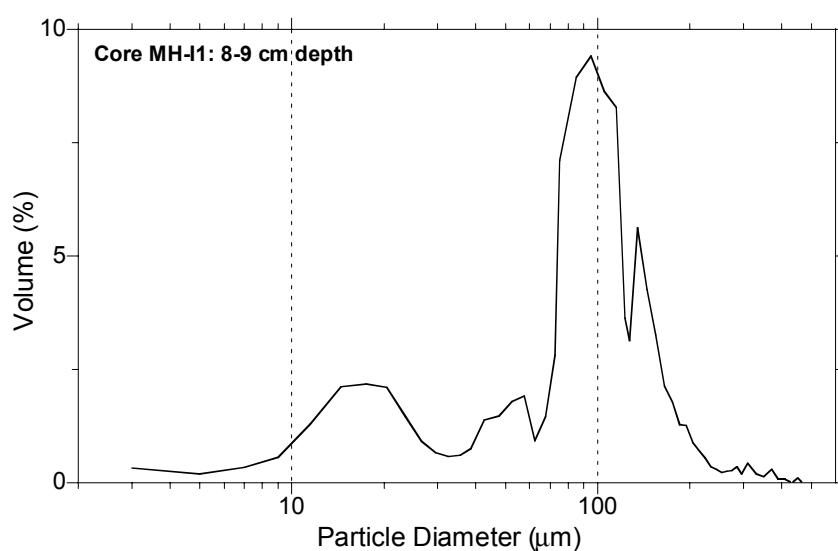


Figure 3.2: Particle size distribution (volume %) of sediment sample from Mahurangi intertidal core MH-I1 (depth: 8–9-cm).

Profiles of median particle diameter (D_{50}) show negligible variations with depth in the sediment column and between replicate cores or between intertidal (Figs. 3.3a) and sub-tidal (Figs. 3.4a) sub-environments. The D_{50} of the Mahurangi intertidal and sub-tidal sediment cores are typically ~100 μm . By comparison, the mud content (%) of the sediment cores show clear spatial variations between core sites and sub-environments (Figs. 3.3b and 3.4b). On the intertidal flat, mud content increases from ~5% (core MH-I3) to 20–40% (core MH-I1) with distance towards the head of the estuary. The depth profiles of mud content in the sub-tidal cores display more complex patterns, with maximum between-site variations occurring at the top and

base of the sediment cores. In neither sub-environment is there a clear trend in particle size from the base to the top of the sediment cores.

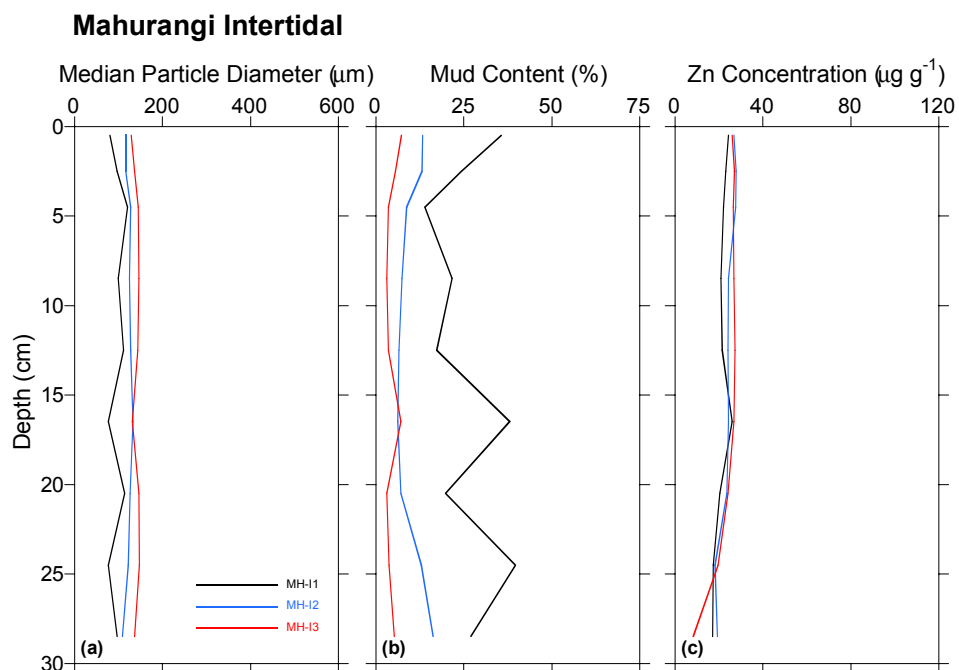


Figure 3.3: Mahurangi intertidal cores (a) median particle diameter, (b) mud content and (c) Zn concentration profiles.

Figures 3.3c and 3.4c show the Zn profiles for the $<2000 \mu\text{m}$ particle size fraction, which are similar in both sub-environments. The range of Zn concentrations in the sub-tidal ($24\text{--}31 \mu\text{g g}^{-1}$) and intertidal ($17\text{--}26 \mu\text{g g}^{-1}$) are similar. In the intertidal cores, small apparent increases in Zn concentrations between the base and top of the cores are within the $\pm 5 \mu\text{g g}^{-1}$ measurement uncertainty. The Zn concentrations measured in the Mahurangi sediment cores are within the range of pre-urbanised “background” values of $10\text{--}30 \mu\text{g g}^{-1}$ previously measured in Auckland estuaries (e.g., Williamson et al. 1998, Craggs et al. 2001, Swales et al. 2002).

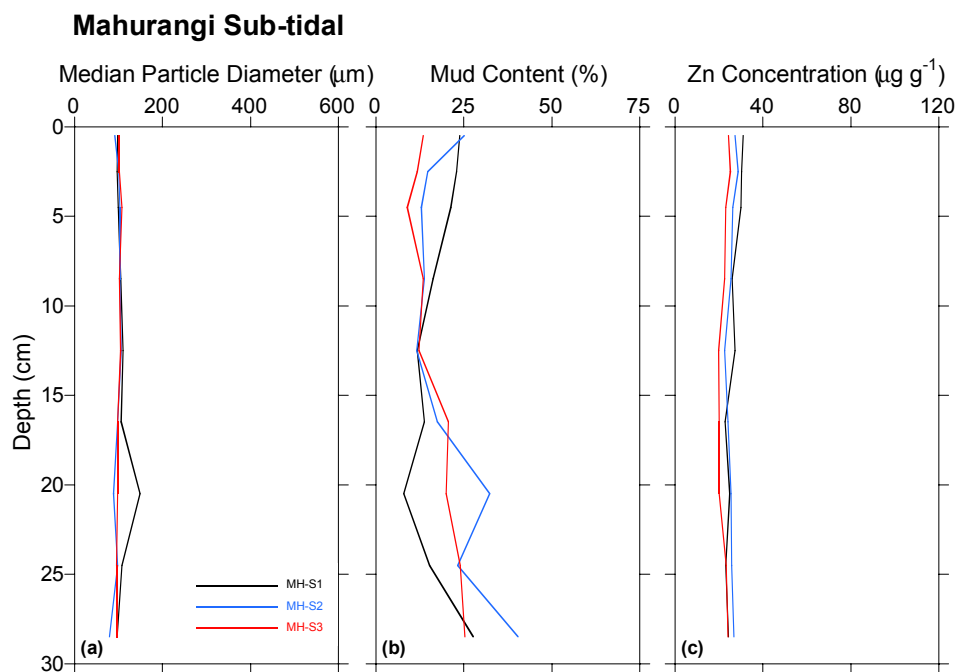


Figure 3.4: Mahurangi sub-tidal cores (a) median particle diameter, (b) mud content and (c) Zn concentration profiles.

3.2.3 Mahurangi recent sedimentation history

Intertidal cores

The Mahurangi intertidal sediment cores contain large quantities (> 40%) of tree fern spores. This indicates that eroded catchment soils are a primary source of pollen and spores in these cores. The intertidal cores preserve a clearer pollen record than the sub-tidal cores, where the presence of recent flora, such as pine, deep in the cores indicates substantial sediment mixing. Core MH-I1 shows a typical pollen record for the intertidal cores with the 1950 and 1980 time horizons indicated (Fig. 3.5). It can be seen that pine and exotic grasses pollen abundance rapidly increases towards the surface of the sediment core, while bracken spore content declines. Appendix II provides detailed pollen and spore data for each of the intertidal and sub-tidal cores.

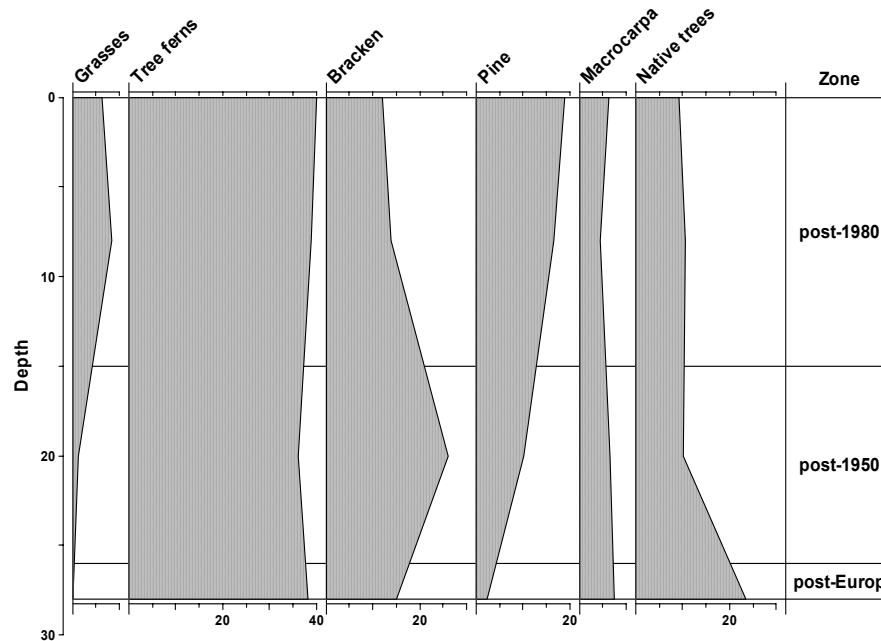


Figure 3.5: Mahurangi estuary intertidal core MH-I1 pollen and spore profiles for major plant groups expressed as percentage of terrestrial pollen and spore sum.

Figure 3.6 shows the ^{137}Cs concentration profiles for each intertidal core, which show maximum ^{137}Cs occurrence between 20-cm and 29-cm. The presence of ^{137}Cs at the sediment surface indicates on-going delivery of ^{137}Cs most likely associated with catchment soil erosion.

SAR calculated from the slopes of the linear regression relations fitted to the unsupported ^{210}Pb profiles are shown in Figure 3.7. Also shown is the maximum depth of ^{137}Cs in the cores, which also provides an independent SAR estimate. The presence or absence of pine pollen as well as its concentration (% of total terrestrial pollen sum) in the bottom-most core sediments also provides information about the age of these cores.

In core MH-I1, a large increase in SAR from 1.1 mm yr^{-1} to 9.4 mm yr^{-1} above 16.5-cm depth is indicated by an abrupt change in slope of the ^{210}Pb profile. The ^{137}Cs -derived SAR of 5.4 mm yr^{-1} is similar to the average of the two ^{210}Pb SAR values. The ^{210}Pb SAR in the top layer indicates that the upper 16.5 cm of the core has been deposited in the last 18 years. The ^{210}Pb SAR of 1.1 mm yr^{-1} for the bottom layer is too low given

that 12 cm of sediment was deposited in this layer, along with ^{137}Cs , after 1953. A possible explanation for the abrupt change in slope of the ^{210}Pb profile is deep mixing of the sediment column by benthic fauna to ~17 cm depth and one-dimensional modelling of deep biological mixing can create similar abrupt changes in the ^{210}Pb profile observed in core MH-I1 (Dr Samuel Bentley, Oceanography Department, Louisiana State University, pers. comm. July 2003). However, these sediments are dominated by herbivorous worms, which graze down to a maximum depth of ≤ 5 cm (Lundquist et al. 2003) and bioturbation alone is unlikely to explain the observed ^{210}Pb profile. An alternative explanation is that the apparent large increase in SAR over the last ~20 years is due to increased net sedimentation. This may reflect a local change in the balance between sediment deposition and re-suspension rather than increased sediment delivery to the estuary. The historical pattern of tidal-channel migration in the vicinity of Hamiltons Landing, where core MH-I1 was taken, reconstructed from deep cores by Swales et al. (1997) could also explain the apparent increase in SAR. The fact that neither cores MH-I2 or MH-I3 have similar ^{210}Pb profiles suggests that the large apparent increase in sedimentation at MH-I1 is due to local sediment dynamics rather than increased sediment delivery to the estuary.

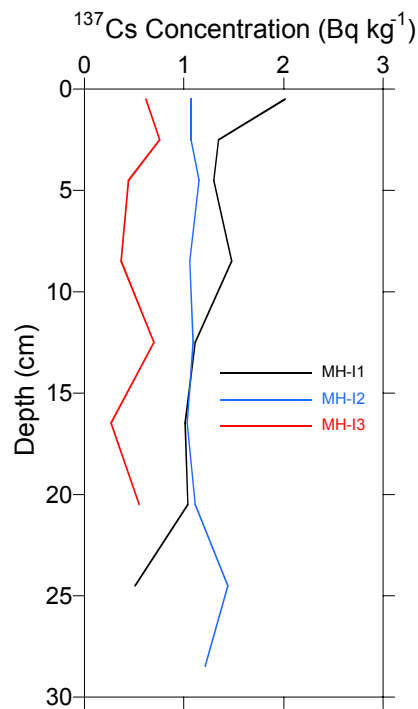


Figure 3.6: ^{137}Cs concentration profiles in the Mahurangi intertidal cores.

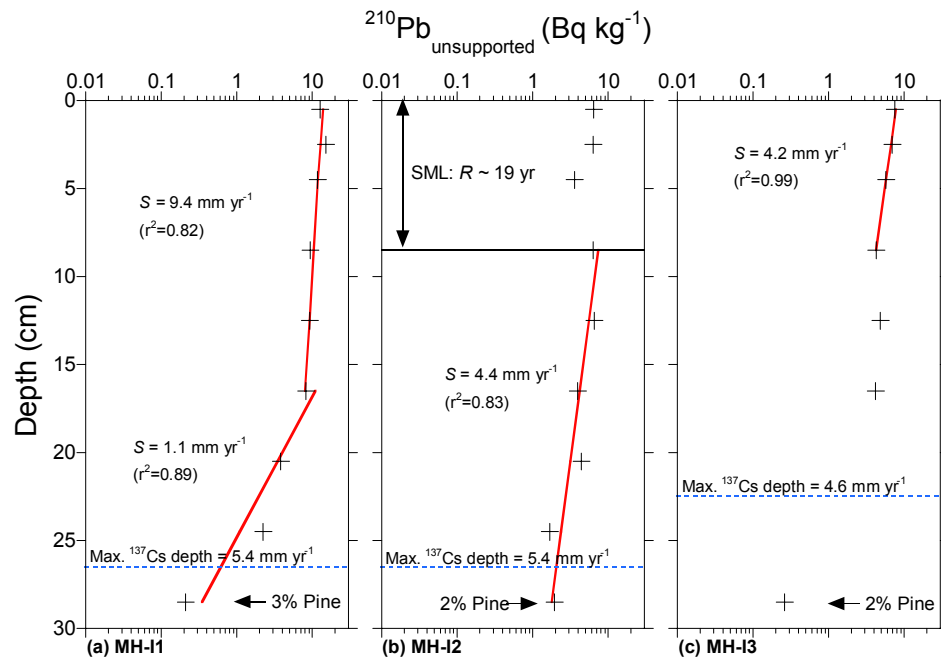


Figure 3.7: Mahurangi intertidal cores. Unsupported ^{210}Pb profiles plotted on a log scale, with linear regression fits used to calculate sedimentation rates (S). Also shown are the surface-mixed layer (SML), associated particle residence time (R) and the maximum depth of ^{137}Cs and average SAR.

Core MH-I2 (Fig. 3.7b) differs markedly from MH-I1. A surface mixed layer (SML) of ~ 8.5 cm is indicated by the relatively uniform ^{210}Pb concentrations in the SML. The ^{210}Pb -derived SAR of 4.4 mm yr^{-1} for the sediments below the SML is similar to the ^{137}Cs -derived SAR of 5.4 mm yr^{-1} . The presence of pine pollen at the base of the core indicates that these sediments have been deposited since the mid-1930's. The particle residence time (R) in the SML, based on the ^{210}Pb SAR is ~ 19 years. Core MH-I3 displays an irregular ^{210}Pb profile, with relatively uniform ^{210}Pb concentrations between 8-cm and 16-cm depth. Fitting a linear regression relation to the top 10-cm of the profile yields a SAR of 4.2 mm yr^{-1} , which is similar to the ^{137}Cs -derived SAR of 4.6 mm yr^{-1} . As in core MH-I2, the presence of pine pollen at the base of the core indicates the upper ~ 30 cm of the sediment column has been deposited since the mid 1930's.

The Mahurangi intertidal cores show substantial between-core differences in their ^{210}Pb profiles while ^{137}Cs -derived SAR ($4.6\text{--}5.4 \text{ mm yr}^{-1}$) are similar. These observations suggest similar average sedimentation rates with local variations in post-deposition sediment mixing.

Figure 3.8 shows the SAR calculated for discrete time-periods from pollen, ^{137}Cs and ^{210}Pb dating. The pollen data indicate that net sedimentation rates on the intertidal flat have increased from $\sim 4 \text{ mm yr}^{-1}$ (1950–1980) to $\sim 7 \text{ mm yr}^{-1}$ since 1980. Comparison of the three dating methods for the post-1950/1953 period shows close agreement, with SAR of 4.2–5.4 mm yr^{-1} .

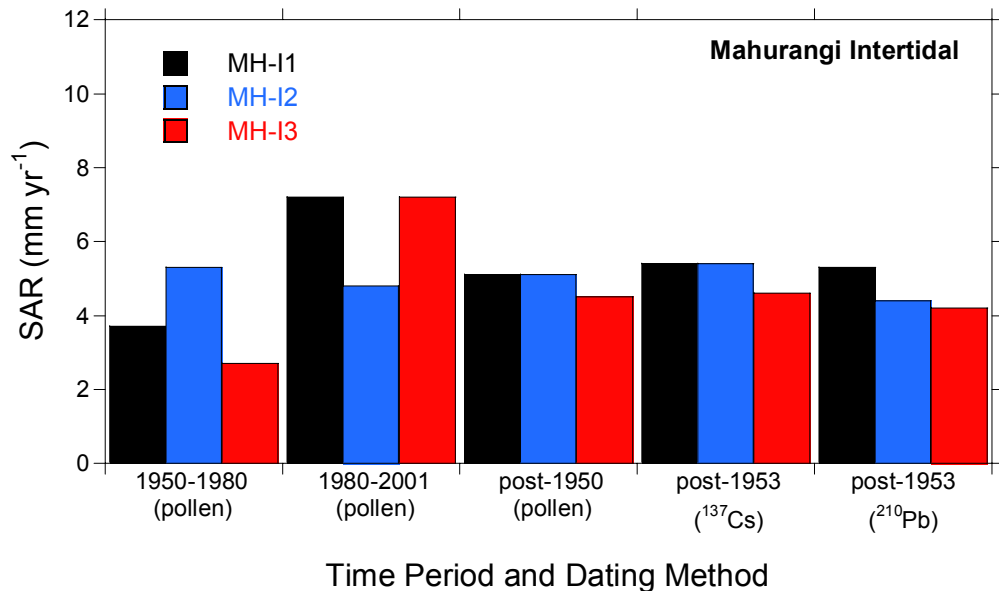


Figure 3.8: Mahurangi intertidal-flat cores, comparison of SAR estimated from pollen, ^{137}Cs and ^{210}Pb dating.

Sub-tidal cores

The sub-tidal cores also contained large quantities of tree fern spores, which is indicative of eroded catchment soils being the primary source of pollen and spores in these cores. The presence of pine, grasses and exotic plants at depth in cores MH-S2 and MH-S3 indicates substantial sediment mixing and it was not possible to determine both the 1950 and 1980 A.D. time horizons in these cores. Figure 3.9 shows the pollen record preserved in core MH-S1. The first detected occurrence of ^{137}Cs to $\leq 20\text{-cm}$ depth (Fig. 3.10) is less than for the intertidal cores.

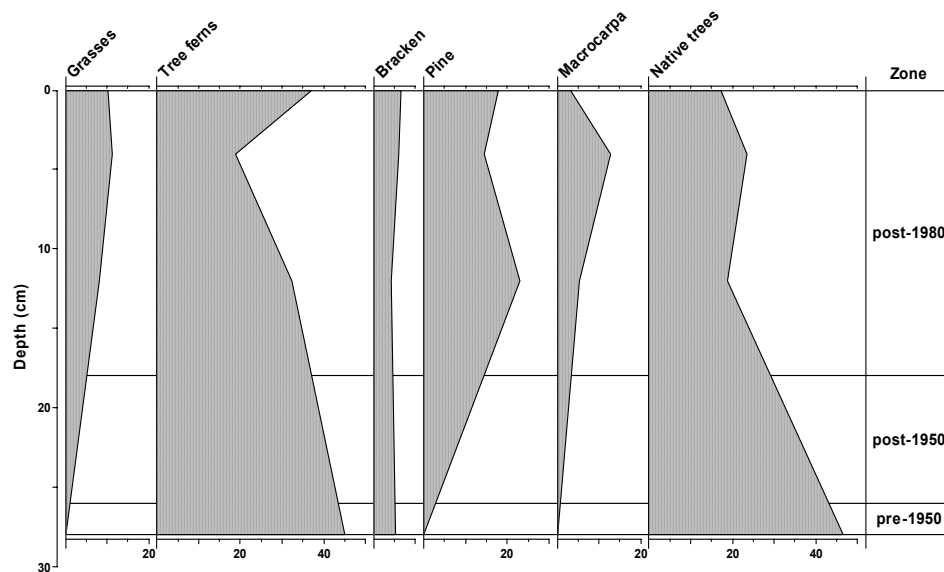


Figure 3.9: Mahurangi estuary sub-tidal core MH-S1 pollen and spore profiles for major plant groups expressed as percentage of terrestrial pollen and spore sum.

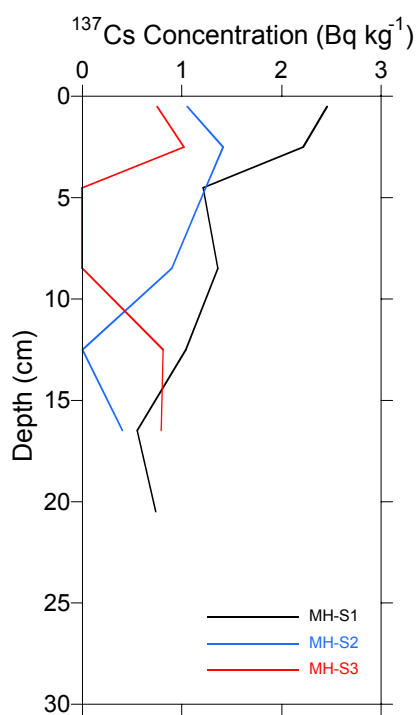


Figure 3.10: ¹³⁷Cs concentration profiles in the Mahurangi subtidal cores.

The subtidal ^{210}Pb profiles also indicate substantial sediment mixing (Fig. 3.11). Uniform ^{210}Pb concentrations occur in the upper 9-cm and 5-cm of cores MH-S1 and MH-S2 respectively. No interpretation of the ^{210}Pb profile in core MH-S3 is possible because of sediment mixing. In core MH-S1, the substantial difference between the ^{210}Pb (1.4 mm yr^{-1}) and ^{137}Cs - derived SAR (4.6 mm yr^{-1}) likely reflect deep sediment mixing. For example, ^{137}Cs deposited in 1953 may have been rapidly mixed (i.e., over several years) to $\sim 9\text{-cm}$ depth (i.e., same as present day SML). Thus the actual maximum depth of ^{137}Cs in the absence of mixing would be $22.5 \text{ cm} - 9 \text{ cm} = \sim 14\text{cm}$, which yields a SAR of 2.9 mm yr^{-1} . Similarly, in core MH-S2 the mixing-corrected maximum depth of ^{137}Cs would be 6 cm , rather than 10.5 cm , which yields a SAR of 1.2 mm yr^{-1} instead of 2.1 mm yr^{-1} and more similar to the ^{210}Pb SAR of 1.5 mm yr^{-1} . The residence time of sediment particles in the SML is of the order of several decades.

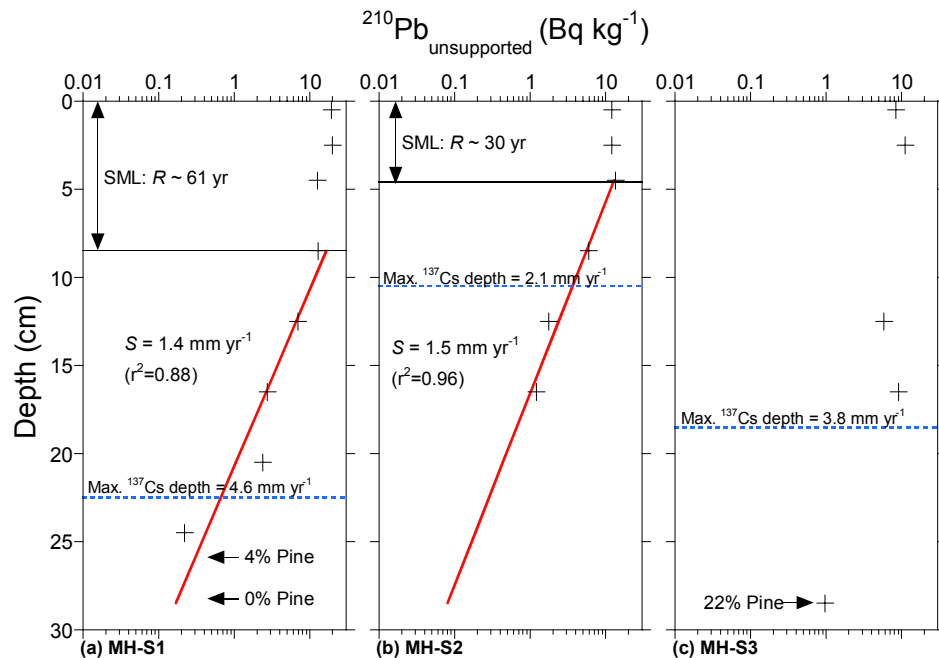


Figure 3.11: Mahurangi subtidal cores. Unsupported ^{210}Pb profiles plotted on a log scale, with linear regression fits used to calculate sedimentation rates (S). Also shown are the surface-mixed layer (SML), associated particle residence time (R) and the maximum depth of ^{137}Cs and average SAR.

Pollen-derived SAR for core MH-S1 indicates a four-fold increase from $\sim 2 \text{ mm yr}^{-1}$ (1950–1980) to $\sim 8 \text{ mm yr}^{-1}$ (1980–2001) (Fig. 3.12). However, SAR calculated using pollen, ^{137}Cs and ^{210}Pb profiles show substantial between-core variations, which likely reflects sediment mixing. These cores were taken from a horse-mussel (*Atrina*

zelandica) bed. *Atrina* are large, long-lived filter-feeding bivalves, which locally influence hydrodynamics and sediment transport. The average lengths of *Atrina* measured at several subtidal sites in the Mahurangi estuary are 20–23 cm, most of which (12–15 cm) is buried in the sediment column (Thrush et al. 1998). Although *Atrina*, as filter feeders, do not actively mix the sediment column, ‘new’ sediment deposited inside their open valves after death would inject sediment to depth in the sediment column. This process repeated over years–decades could be an effective mixing process. Alternatively, the burrowing activities of animals living in the *Atrina* sediments (Lundquist et al. 2003) could also mix the upper sediment column. Consequently, there is poor consistency of SAR between sites and dating methods.

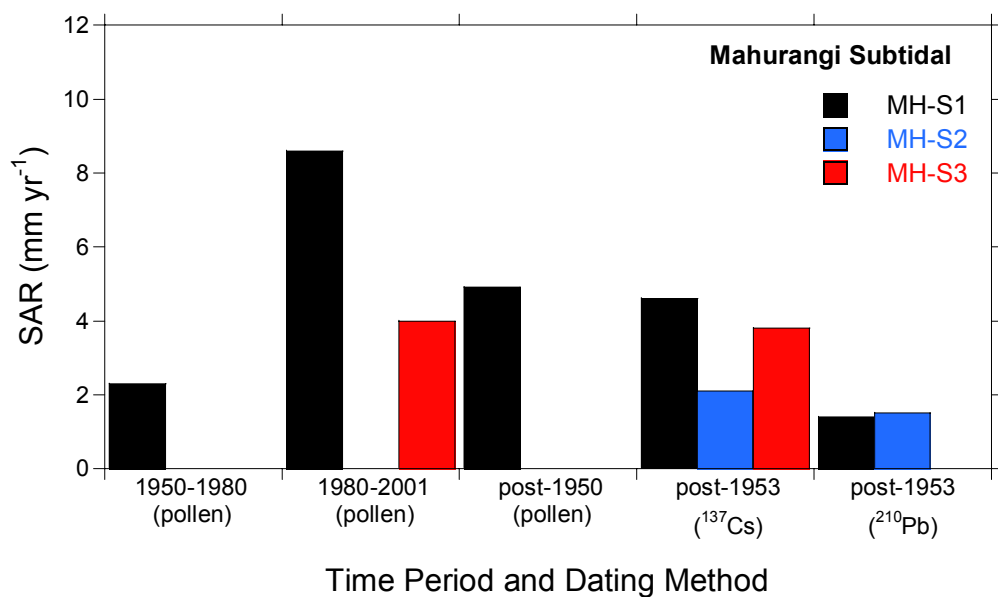


Figure 3.12: Mahurangi subtidal-flat cores, comparison of SAR estimated from pollen, ¹³⁷Cs and ²¹⁰Pb dating.

3.3 Puhoi estuary (intertidal cores)

3.3.1 Background

The Puhoi estuary is one of several similar tidal-lagoon estuaries that fringe Auckland’s east coast north of the Whangaparaoa Peninsula (Fig. 3.13). The estuary is sheltered from the sea by a large sand barrier at its mouth that has been constructed by wave action. The Puhoi estuary has a high-tide surface area of 1.7 km² and a tidal

prism of $2.7 \times 10^6 \text{ m}^3$ or ~6% of the tidal volume of the Mahurangi estuary (Table 3.1). The estuary is substantially infilled with sediment (i.e., ~70% intertidal) and a quarter of the total estuary area has been colonised by mangrove. The main tidal channel is braided in the lower estuary with extensive intertidal sand flats, which become increasingly muddy with distance towards the head of the estuary. Because the estuary is largely intertidal (Table 3.1), there is almost complete exchange of estuarine water with each tidal cycle. The estuary receives runoff from a 43-km² catchment.

Catchment landcover originally consisted of an undisturbed, mixed conifer-hardwood forest dominated by rimu, kahikatea, totara, matai and miro. Catchment deforestation began in the 1860's with the arrival of Bohemian settlers. By the late 1870's much of the original forest landcover had been replaced by pasture and in the 1920's and 1930's dairy farming was prevalent (Haworth, 1994). Planting of several hundred hectares of *P. radiata* forest in the upper catchment occurred in 1974–1978 and logging of the first rotation began in the late 1990's (Simon Anderson CHH Forests Northern Region, pers comm.). Present day catchment landcover is comprised of regenerating native forest (20%) and scrub (10%), production forestry (23%) and pasture (47%) (source: NZ Land Resource Inventory).

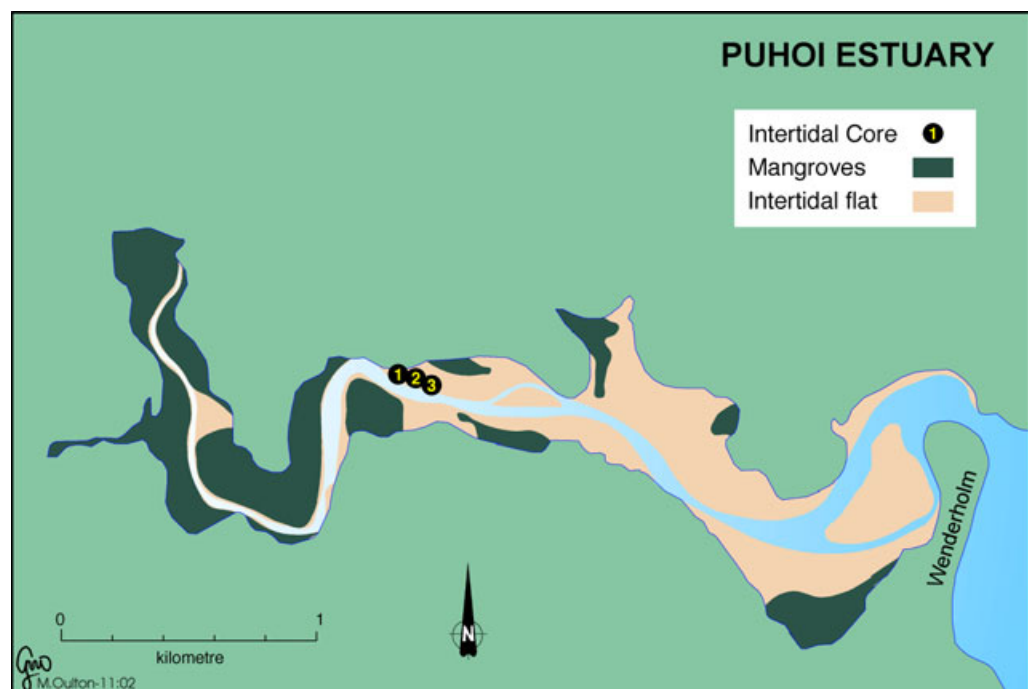


Figure 3.13: Puhoi estuary - location of intertidal cores and major sub-environments.

3.3.2 Puhoi estuary sediments

Replicate sediment cores were collected from an intertidal mud flat in the upper reaches of Puhoi estuary adjacent to a channel meander. The core sites were ~100-m apart and parallel to the main tidal channel (Fig. 3.13). The mud flat forms a discrete lobe beginning at the outside bank of the channel meander and extending several hundred metres towards the mouth of the estuary (Fig. 3.14). These sediments are mixtures of fine silt (~20 μm modal diameter) and very-fine sand (~100–150 μm modal diameter) as described for the Mahurangi estuary. Dry bulk sediment densities (1.1–1.7 g cm^{-3}) are similar in all cores and the profiles display a gradual trend of increasing density with depth (Appendix III).



Figure 3.14: Puhoi estuary, view looking towards the estuary mouth from core site PU-I1.

Profiles of D_{50} for the Puhoi cores show negligible variation between sites or with depth in the sediment column and median particle diameters range between 110–150 μm (Fig. 3.15a). The mud content of the cores varies between 5 and 20% and shows no clear pattern (Fig. 3.15b).

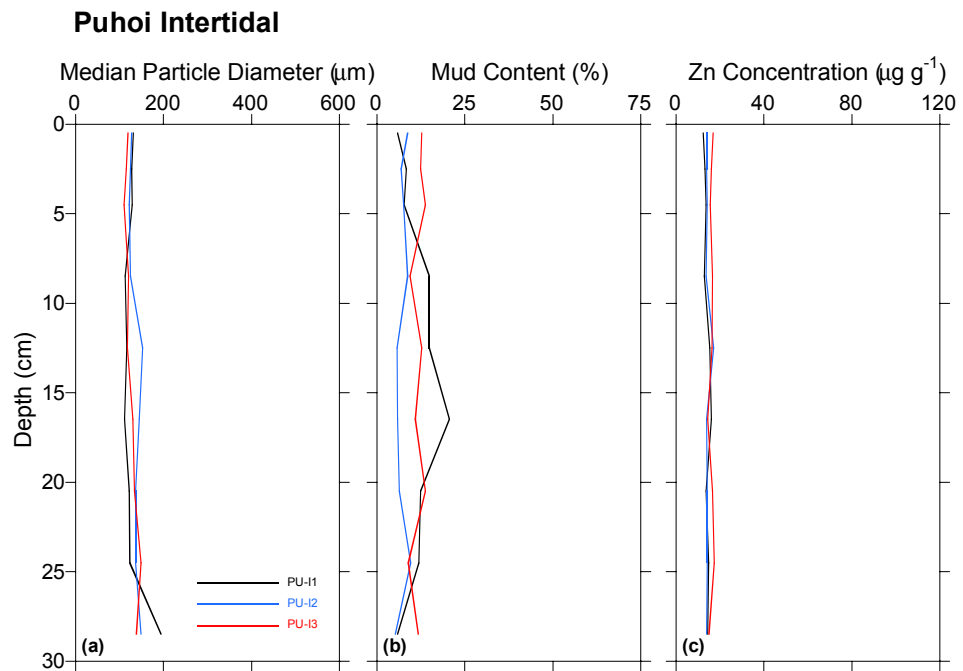


Figure 3.15: Puhoi intertidal cores (a) median particle diameter, (b) mud content and (c) Zn concentration profiles.

Zn concentration profiles are near identical in all three Puhoi cores. The Zn concentrations vary between 12–17 $\mu\text{g g}^{-1}$ (Fig 15c), which is within the range of pre-urban “background” values (i.e., 10–30 $\mu\text{g g}^{-1}$) for Auckland estuaries (e.g., Williamson et al. 1998, Craggs et al. 2001, Swales et al. 2002).

3.3.3 Puhoi recent sedimentation history

The pollen assemblages contained in the Puhoi estuary cores are dominated by tree fern spores (60–80%), which is a strong indication that these sediments are derived from eroded catchment soils (Fig 3.16).

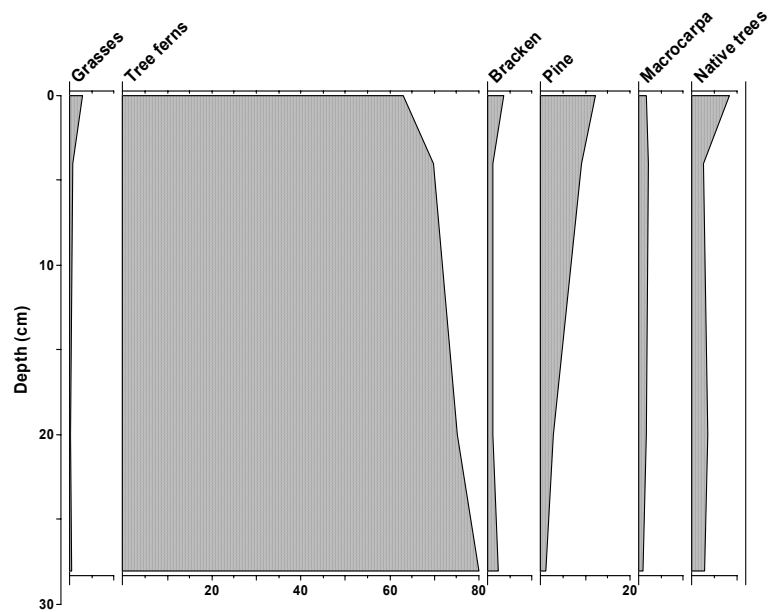


Figure 3.16: Puhoi estuary intertidal core PU-I1 pollen and spore profiles for major plant groups expressed as percentage of terrestrial pollen and spore sum.

The high tree-fern content precludes accurate pollen dating of these sediments. The presence of ^{137}Cs to the base of cores PU-I1 and PU-I3 indicates that these sediments have been deposited since 1953 (Fig. 3.17). Consequently, the ^{137}Cs -derived SAR of 5.9 mm yr^{-1} is a minimum value. In core PU-I2, maximum ^{137}Cs depth to 26.5 cm yields a SAR of 5.4 mm yr^{-1} . The location and orientation of the mud deposit, as well as the fine-grained sediment texture, and the high tree-fern spore content suggest that these sediments were delivered in suspension and deposited during catchment floods.

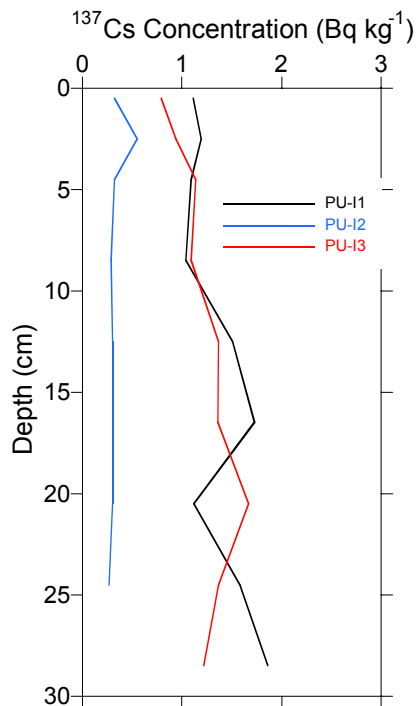


Figure 3.17: ¹³⁷Cs concentration profiles in the Puhoi intertidal cores.

The ²¹⁰Pb profiles suggest that sedimentation in the upper Puhoi estuary has been relatively rapid (Fig. 3.18). In core PU-I1, a SAR of ~28 mm yr⁻¹ is similar to values measured in the upper reaches of the Mahurangi, Pakuranga and Mangemangeroa estuaries (Swales et al. 1997, Oldman and Swales 1999, Swales et al. 2002). The presence of ¹³⁷Cs at the base of core PU-I1 shows that the SAR is ≥5.9 mm yr⁻¹, but we cannot confirm the ²¹⁰Pb SAR by pollen or ¹³⁷Cs dating. The *r*² value (0.2) for the regression fit to the ²¹⁰Pb data is also low. In core PU-I2 the ²¹⁰Pb-derived SAR of 4.1 mm yr⁻¹ is similar to the ¹³⁷Cs SAR (5.4 mm yr⁻¹) so that we can have some confidence in the dating. The ²¹⁰Pb SAR for core PU-I3 of 9.8 mm yr⁻¹ cannot be validated because ¹³⁷Cs and pine pollen both occur in basal sediments. The rapid sedimentation indicated by the ²¹⁰Pb, ¹³⁷Cs and pollen profiles is consistent with flood sedimentation of catchment soils on an intertidal flat adjacent to a channel meander.

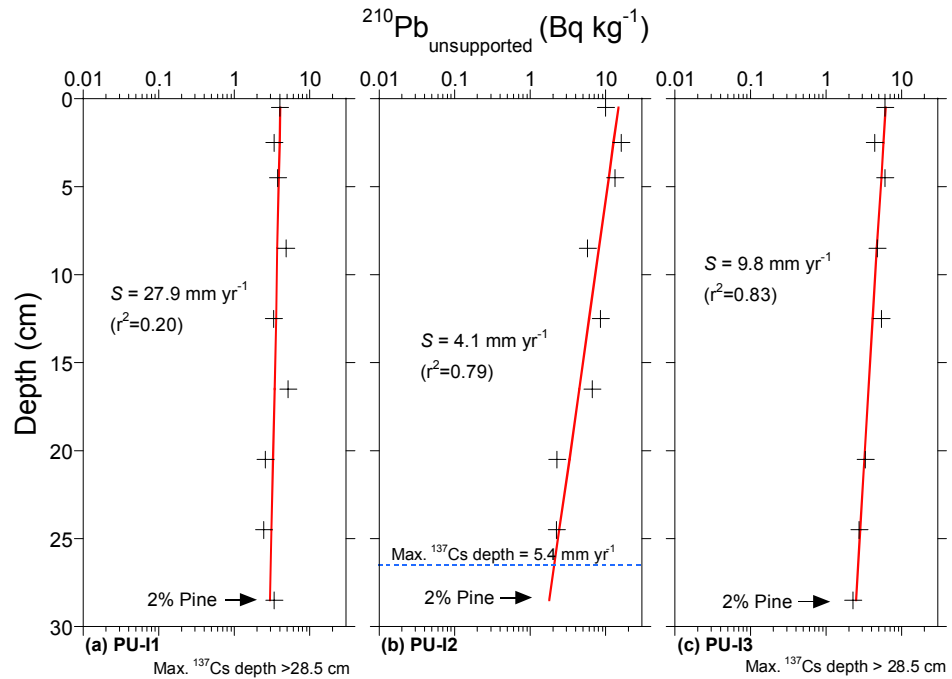


Figure 3.18: Puhoi intertidal cores. Unsupported ^{210}Pb profiles plotted on a log scale, with linear regression fits used to calculate sedimentation rates (S). Also shown, for core PU-I2, is the maximum depth of ^{137}Cs and average SAR.

3.4 Okura estuary (intertidal cores)

3.4.1 Background

The Okura estuary is a small (Table 3.1), infilled drowned valley estuary, which opens to the sea in the southern lee of Whangaparoa Peninsula (Fig. 3.19). The estuary has a high-tide surface area of 1.4 km² and a tidal prism of only ~5% of the Mahurangi estuary.

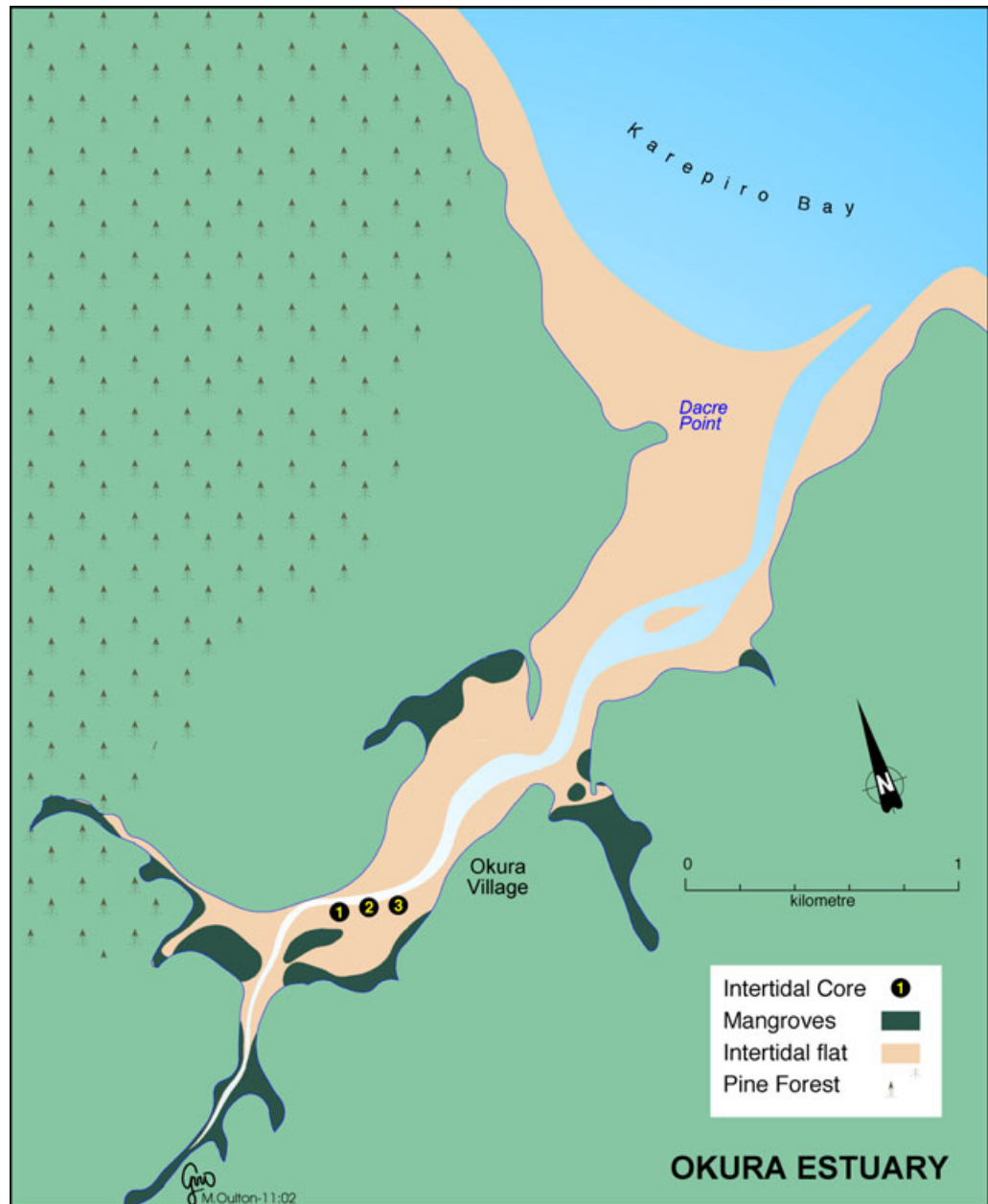


Figure 3.19: Okura estuary - location of intertidal cores and major sub-environments.

The Okura estuary has a single main tidal channel flanked on both sides by an intertidal flat, which are submerged to an average depth of 1 m (Green and Oldman 1999). The estuary is funnel-shaped and its width, which is ~0.6 km at the mouth, rapidly diminishes towards the head of the estuary. In the middle estuary a shell spit, some 300-m long, extends across the intertidal flats from the northern shore. Seaward of the spit, intertidal sediments are sandy whereas above the spit the intertidal flats become increasingly muddy. The upper estuary is also fringed by extensive stands of mangrove. Because the estuary is largely intertidal, there is

almost complete exchange of estuarine water with each tidal cycle. The estuary receives runoff from a 22.7-km² catchment.

The original catchment landcover was likely to be similar to the nearby Mahurangi catchment, which consisted of an undisturbed, mixed conifer-hardwood forest dominated by rimu, kahikatea, totara, matai and miro. European settlement from the mid-1800's brought about rapid deforestation in the Mahurangi, Puhoi and Waitemata estuary catchments (Haworth, 1994; McGlone, 1994; Schriener, 1981) and the deforestation of the Okura estuary is likely to have a similar history. Pine species, including *P. radiata* and *P. pinaster* were originally planted in the mid-1940's by the Haig family, although the total area planted was not more than several hectares (Mrs T. McKay, Okura resident pers. comm., November 2002). Planting of a ~300 ha *P. radiata* forest at Wiet Station, adjoining the northern shore of the estuary, began in the early 1970's. A clear signature of the pine forest planting should be evident in the stratigraphic record, given the close proximity and the size of the forest. Present day catchment landcover is dominated by native forest and scrub (43% area) and pasture (40% area) (Stroud et al. 1999). As urban development and rural intensification continues, further landcover changes are anticipated. Construction of the Okura section of Albany–Puhoi highway occurred in 1998 and much of the Okura catchment is potentially available for rural intensification (Stroud et al. 1999).

3.4.2 Okura estuary sediments

Replicate sediment cores were collected from an intertidal flat in the upper reaches of Okura estuary and in close proximity to the pine plantation on the northern flank of the estuary (Fig. 3.19). The core sites were ~150-m apart and parallel to the main tidal channel (Fig. 3.20). Intertidal sediments are typically muddy fine sands composed of fine silt (~20 µm modal diameter) and very fine sand (~100–150 µm modal diameter) similar to the Mahurangi estuary. Dry bulk sediment densities in the cores vary between 1.0–1.8 g cm⁻³ (Appendix III).

Profiles of D_{50} for the Okura cores show negligible variation in median particle size between sites. The typical range of D_{50} is 100–120 µm (Fig. 3.21a). However, in the top-most 5-cm of the sediment column there is a reduction in D_{50} values, which is most evident in OK-I1 (most landward site). At this core site, D_{50} halves from 128µm at 4–5 cm depth to 61µm in the surface sediments. Similar patterns are displayed by the mud content (%) data. Below 5-cm depth the mud content of sediments in all three cores are in the range 5–20% (Fig. 3.21b). In core OK-I1, the mud content of

sediments increases from 18 to 54% in the upper 5 cm of the sediment column. Smaller increases are indicated for the other two cores. The Galai data show a change from muddy fine sands to increasingly muddy sediments in the top 5 cm of the sampled intertidal flat.



Figure 3.20: Okura estuary, view looking towards the head of the estuary. Sediment cores taken from the intertidal flat to the left of the channel. Core OK-I3 taken opposite the orange buoy and ~20-m upstream.

Zn concentrations have similar ranges in all the cores and increase from 12–14 $\mu\text{g g}^{-1}$, at the base of the core, to 21–24 $\mu\text{g g}^{-1}$ in surface sediments (Fig. 3.21c). In OK-I1, Zn concentration profile shows an increase of 16–24 $\mu\text{g g}^{-1}$ in the top-most 10 cm of the core, however the increase is within the estimated uncertainty of the analytical method. Zn concentrations in these sediments are within the range of pre-urbanised “background” values (i.e., 10–30 $\mu\text{g g}^{-1}$) for Auckland estuaries (e.g., Williamson et al. 1998, Craggs et al. 2001, Swales et al. 2002).